Environmental Pollution 278 (2021) 116821

Contents lists available at ScienceDirect

Environmental Pollution

journal homepage: www.elsevier.com/locate/envpol

Responses of juvenile fathead minnow (*Pimephales promelas*) gut microbiome to a chronic dietary exposure of benzo[*a*]pyrene☆

Abigail DeBofsky [a], Yuwei Xie [a, *], Jonathan K. Challis [a], Niteesh Jain [a], Markus Brinkmann [a, b, c], Paul D. Jones [a, b], John P. Giesy [a, d, e]

[a] Toxicology Centre, University of Saskatchewan, Saskatoon, Saskatchewan, Canada
[b] School of Environment and Sustainability, University of Saskatchewan, Saskatoon, Saskatchewan, Canada
[c] Global Institute for Water Security, University of Saskatchewan, Saskatoon, Saskatchewan, Canada
[d] Department of Veterinary Biomedical Sciences, University of Saskatchewan, Saskatoon, Saskatchewan, Canada
[e] Department of Environmental Science, Baylor University, Waco, TX, USA

ARTICLE INFO

Article history:
Received 12 September 2020
Received in revised form
10 February 2021
Accepted 20 February 2021
Available online 25 February 2021

Keywords:
Homeostasis
Next-generation sequencing
Persistent organic pollutants
Fish
Metagenomics
16s rRNA metagenetics

ABSTRACT

The microbiome has been described as an additional host "organ" with well-established beneficial roles. However, the effects of exposures to chemicals on both structure and function of the gut microbiome of fishes are understudied. To determine effects of benzo[*a*]pyrene (BaP), a model persistent organic pollutant, on structural shifts of gut microbiome in juvenile fathead minnows (*Pimephales promelas*), fish were exposed *ad libitum* in the diet to concentrations of 1, 10, 100, or 1000 μg BaP g^{-1} food, in addition to a vehicle control, for two weeks. To determine the link between exposure to BaP and changes in the microbial community, concentrations of metabolites of BaP were measured in fish bile and 16S rRNA amplicon sequencing was used to evaluate the microbiome. Exposure to BaP only reduced alpha-diversity at the greatest exposure concentrations. However, it did alter community composition assessed as differential abundance of taxa and reduced network complexity of the microbial community in all exposure groups. Results presented here illustrate that environmentally-relevant concentrations of BaP can alter the diversity of the gut microbiome and community network connectivity.

1. Introduction

The gut microbiome is a crucial component of an animal host and is responsible for a number of important biological processes, including energy and nutrient cycling (Dimitroglou et al., 2011), regulation of intestinal barrier functions (Pérez et al., 2010), and modulation of the immune system (Rolig et al., 2015). Disturbance of structure of the gut microbiome is associated with several harmful effects, including inflammatory bowel disease, metabolic syndromes, stress, and disease (Carding et al., 2015; He et al., 2019; Llewellyn et al., 2014). Although considerable research efforts to understand links between xenobiotics and gut microbiome have been conducted in mammals (i.e., Breton et al., 2013; Lefever et al., 2016; Ribière et al., 2016), the effects of toxicants on gut microbial community structure and function in fish are largely unknown.

Complex interactions between the host microbiome and xenobiotics can vary by route of exposure. In fish, due to partitioning and bioaccumulation, exposure to environmental toxicants can occur *via* multiple routes and transport of persistent organic pollutants (POPs) tend to accumulate in food chains (Schlenk et al., 2008; Wang and Wang, 2006). POPs can be taken up through the gut, skin, and gill, and can ultimately have deleterious effects on fish in freshwater ecosystems. The mucosal layers of the skin, gill, and gut all contain microbiomes that provide protective barriers for fish defense against pathogens (Salinas and Magadán, 2017) and serve as an intermediary in the metabolism pathway of some toxicants (Adamovsky et al., 2018).

Benzo[*a*]pyrene (BaP) is a promising model polycyclic aromatic hydrocarbon (PAH) to study the potential effects of toxicants on the gut microbiome because much is known about its effects in the host but little on the microbiome. BaP originates from sources such as the incomplete combustion of fossil fuels and oil spills (Srogi, 2007) and has well-characterized deleterious effects in fishes (Carlson et al., 2004a; Costa et al., 2011; Nacci et al., 2002; Phalen et al.,

☆ This paper has been recommended for acceptance by Dr. Sarah Harmon.
* Corresponding author.
E-mail address: yuwei.xie@usask.ca (Y. Xie).

https://doi.org/10.1016/j.envpol.2021.116821
0269-7491/

2014). BaP up-regulates the expression of cytochrome P450 1A (CYP1A), which results in the biotransformation of BaP to reactive intermediates (Ortiz-Delgado et al., 2007). Adverse outcomes of exposure to BaP include the development of lesions and tumors, as well as suppression of immune function (Beyer et al., 2010; Carlson et al., 2004b; Tuvikene, 1995). Conjugated products from phase II metabolism of BaP often end up in the bile of exposed fish (Nishimoto et al., 1992). In fish, routes of exposure to BaP are primarily through ingestion with food, incidental ingestion of sediment, dermal contact, and *via* ventilation across the gills (Mccarthy et al., 2003; Nichols et al., 1996; Snyder et al., 2015; Tuvikene, 1995). Route of exposure is a critical component of the distribution of BaP. For example, aqueous exposure of BaP in rainbow trout (*Oncorhynchus mykiss*) results in detectable BaP throughout the body, while dietary exposure mainly results in accumulation of BaP in the bile and intestine (Sandvik et al., 1998).

Effects of BaP on the structure and function of the gut microbiome of fishes are not well studied. Aqueous exposures of adult fathead minnows to small concentrations of BaP resulted in an enrichment of taxa associated with hydrocarbon degradation and community compositional shifts (DeBofsky et al., 2020a), and aqueous exposure of Japanese sea cucumbers (*Apostichopus japonicus*) to BaP resulted in fewer bacteria associated with beneficial functions within the host accompanied by an increase in alkane-degrading bacteria (Zhao et al., 2019). BaP exposure also induced dysbiosis of the microbiome and inflammation of adult western mosquitofish and zebrafish (Xie et al., 2020). Furthermore, concentrations of PAHs in dorsal muscle after an oil spill correlated with gut community composition in walleye (*Sander vitreus*) and with several families of bacteria within the gut microbiome of other species of wild fish (DeBofsky et al., 2020b). However, since the gut microbiome of fishes might be shaped by morphological changes during development, at least in a controlled environment (Yan et al., 2016), there is still a knowledge gap of the effects of BaP on gut microbiomes of juveniles.

This study assessed effects of the gut microbiome in juvenile fathead minnows to dietary BaP exposure. A limited duration exposure *via* the diet can directly deliver BaP into the intestines at comparably greater concentrations than *via* aqueous routes. Specific objectives of this study were to: 1) Characterize the fathead minnow gut microbiome in juvenile fathead minnows; 2) Measure bile metabolites resulting from exposure to BaP; 3) Characterize effects of BaP on the microbiome in guts of fish exposed to BaP, relative to that of unexposed controls; 4) Compare shifts in the microbiome to measured concentrations of BaP metabolites in bile. To satisfy these objectives, microbiomes in guts of fathead minnows were characterized using 16S rRNA metabarcoding after dietary exposure to BaP for two weeks.

2. Materials and methods

2.1. Fish husbandry, dietary exposure, and sampling

Juvenile fathead minnows of approximately 2.5 months of age were obtained from an in-house stock population of the Aquatic Toxicology Research Facility at the University of Saskatchewan. After a one-week acclimation, fish were randomly assigned to each group ($n = 10$ fishes per tank; 3 tanks per group) and were exposed to a solvent control (0.02% methanol, the solvent carrier for BaP), or nominal concentrations of 1, 10, 100, or 1000 μg BaP g^{-1} in food (dry mass, dm) for two weeks. Food was prepared by adding a solution of BaP to the food and allowing the methanol to evaporate. Tanks were siphoned daily to remove excess food and waste. Nominal concentrations were based on environmentally-relevant, albeit extreme, concentrations of PAHs found in fish prey at contaminated sites. For instance, in Norway, concentrations in tissues of the common limpet (*Patella vulgate*), a marine mollusk, were observed to be as great as 15 μg PAHs g^{-1} (Knutzen and Sortland, 1982) while 303 μg PAHs g^{-1} has been measured in tissues of mussels from the French coast (Claisse, 1989). In sediments, concentrations as great as 142 μg PAHs g^{-1} in Puget Sound (Malins et al., 1987), and 7283 μg PAHs g^{-1} have been reported in weathered creosote-contaminated sediment in Eagle Harbor, Washington (Neff et al., 2005). Thus dietary exposures could be as great as these concentrations (Silva et al., 2008). BaP was chosen as a model compound for PAH due to its persistence, mode of action, and relatively well-studied background. Additionally, because PAHs are rapidly metabolized, utilizing high concentrations would allow for accumulation of comparable concentrations in the bile as would be found in contaminated sites (Ohiozebau et al., 2016). At the end of the exposure, fish were euthanized *via* blunt force. Whole-body mass and total length were measured prior to dissection. Samples of whole gut, containing both tissues of the fish and adherent microbes, were excised from all fish. Gallbladders were also removed for quantification of BaP metabolites. If fish showed development of gonads, sex was recorded. Samples were placed in sterile cryovials, and held in liquid nitrogen until storage in a −80 °C freezer. All fish were maintained following the animal use protocol (Protocol #20090108) approved by the Animal Research Ethics Board at the University of Saskatchewan. The detailed methods for fish husbandry are described in the Supporting Information (SI) Text S1.

2.2. Quantification of BaP in food

To quantify BaP in food, an internal calibration and isotope dilution were used to quantify BaP in samples using an eight-point calibration curve between 0.5 and 500 ng BaP mL^{-1}, each containing 100 ng ml^{-1} with BaP-d12. Pressurized liquid extraction was conducted to extract target compounds. A blank cell (no fish food) was also loaded and extracted to serve as an extraction blank. Quantification of BaP was done by GC-QE-Orbitrap mass spectrometer system (Q Exactive GC, Thermo Scientific, Mississauga, ON) with a Thermo RSH autosampler and a TRACE 1310 GC with a heated split/splitless injector running in splitless mode. For detailed information about the extraction and instrumental analysis methods, please refer to the method section of SI Text S2.

2.3. Relative quantification of metabolites of BaP in bile

A semi-quantitative method was applied due to the lack of available standards for Gluc and SO_4 metabolites of BaP. Concentrations of mono-hydroxylated benzo[a]pyrene (OH−BaP) were quantified directly by use of analytical standards and external calibration. Semi-quantification of OH−BaP−O-glucuronide (BaP-Gluc), and sulfate-BaP (BaP−SO4) was conducted using a relative response factor approach. Detailed methods for quantification can be found in the SI Text S3. Instrument detection limits of OH−BaP were determined using the lowest calibration standard (0.3 ng ml^{-1}) estimated as 3x and 10x the signal-to-noise ratio for the limit of detection (LOD) and limit of quantification (LOQ), respectively. Detection limits for BaP-Gluc and BaP−SO4 had to be estimated from OH−BaP by use of reported response factors, as was done for the bile concentrations (SI Table S1). Given the lack of matched isotopically-labeled standards and the extrapolation of averaged response factors based on a small number of representative bile samples, this data should be treated as semi-quantitative. However, it provides information on the relative concentrations of the major metabolite classes.

2.4. 16S rRNA metabarcoding and bioinformatics

Total DNA was isolated from intestines using the AllPrep DNA/RNA Mini Kit (Qiagen Inc., Mississauga, ON). PCR, construction of the sequencing library, next-generation sequencing, and bioinformatics were performed as described in (DeBofsky et al. (2020a)). Taxonomy was assigned in QIIME2 by use of the feature classifier trained against the SILVA 132 reference database (Bokulich et al., 2018; Quast et al., 2013). On average, 69% of demultiplexed reads survived through the cleaning process. In total, 99% of the cleaned reads aligned to bacteria. A full list of reads per sample pre- and post-cleaning can be found in SI Table S2. To avoid biases resulting from differences in sequencing depth, based on a rarefaction curve (SI Fig. S1), the feature table was rarefied at a depth of 13,133 sequences per sample. Alpha-diversities (Shannon diversity and observed ASVs), or diversity within samples, and beta-diversities (Lozupone and Knight, 2005), or differences between samples, were calculated in QIIME2 (Bolyen et al., 2019). PICRUSt2 (Douglas et al., 2019) was used to predict functional abundances of MetaCyc pathways (Caspi et al., 2017) based on 16S rRNA gene sequences, using default parameters. Data can be accessed at https://dx.doi.org/10.20383/101.0247.

2.5. Statistics

Statistical analyses were performed using the R Statistical Language v. 3.6.1 (R Core Team, 2013). Unless otherwise noted, statistics were calculated using vegan v. 2.5–6 (Oksanen et al., 2019). The distribution of variables was checked and compared between groups following previous pipelines (DeBofsky et al., 2020a). No significant differences in body size or number of ASVs were observed between tanks within each treatment group. Condition factor was calculated as (Equation (1)).

$$\text{Condition Factor } (K) = \frac{\text{Mass } (g)}{\text{Standard Length } (mm)^3} \times 100 \qquad (1)$$

To normalize data, concentrations of BaP metabolites were $\log_{10}$-transformed; to account for the presence of zeros in this data set, an arbitrary value of 0.0001 was given to these zero values. In some cases, volumes of bile were too small to obtain a sufficient response, which resulted in an N/A for those samples. To retain as much microbiome data as possible, empty bile values were assigned an average value from their treatment group (Raghunathan, 2004). Values were removed based on the following criteria: fish showing sexual differentiation or fish of greater masses and/or length (based on outliers determined with boxplots) within each treatment group. Differentially abundant bacterial taxa and MetaCyc pathways were calculated using an ANOVA-Like Differential Expression tool (ALDEx2) v 1.18.0 (Fernandes et al., 2014). ALDEx2 transforms data using Aitchison's centered log-ratio (CLR). Additional Spearman correlations were also computed using CLR-transformed abundances of taxa and MetaCyc pathways. Differences among community compositions based on unweighted and weighted Unifrac distances were assessed using PERMANOVA by use of PRIMER software (v 7). Tank was set as a random factor for ANOVA and PERMANOVA tests. A Constrained Analysis of Principal Coordinates (CAP) was conducted using the capscale function in vegan to ordinate the data and view the clusters of samples. Significant BaP metabolites contributing to the ordination were assessed using an ANOVA. Association networks of abundant amplicon sequence variants (ASVs) within treatment groups were inferred using SparCC (Friedman and Alm, 2012) with 100 bootstraps to assign p-values. Networks were displayed and analyzed with Cytoscape v. 3.8.0 (Shannon et al., 2003).

3. Results

3.1. Concentrations of BaP in food and bile metabolites

Concentrations of metabolites in bile confirmed exposure of fish to BaP. Measured concentrations of BaP in food were close to the nominal concentrations (within 20% relative difference, SI Table S3). Concentrations of bile metabolites ($\log_{10}$-transformed) were significantly different among exposures (Fig. 1). BaP *via* dietary route was rapidly metabolized by juvenile fathead minnows. OH–BaP metabolites, initial oxidation of BaP, had a significantly greater concentration in fish fed 100 and 1000 μg BaP g^{-1} in the diet, relative to other groups (Dunnett's test, $p < 0.001$). Sulfate conjugated metabolite (BaP–SO_4) dominated the bile metabolites. Condition factor of fish was not significantly impacted by exposure to BaP (SI Fig. S2).

3.2. Gut microbiome of juvenile fathead minnows

Gut microbiome of juvenile fathead minnows was dominated by three phyla, for instance, *Fusobacteria* (which included mainly *Fusobacteriia*), *Proteobacteria* (which included mainly *Gammaproteobacteria*), and *Bacteroidetes* (which included mainly *Bacteroidia*) (Fig. 2A and B). The dominant families (±standard error) were *Fusobacteriaceae* (65% ± 1%), *Aeromonadaceae* (19% ± 1%), *Pseudomonadaceae* (3% ± 0.3%), and *Flavobacteriaceae* (3% ± 0.3%) (Fig. 2C). A total of 1309 non-singleton ASVs of 64 unique genera of bacteria among 83 samples (control: $n = 17$; 1 μg BaP g^{-1} food: $n = 16$; 10 μg BaP g^{-1} food: $n = 16$; 100 μg BaP g^{-1} food: $n = 16$; 1000 μg BaP g^{-1} food: $n = 18$) remained after filtering. Filtering removed 67 total samples of the 150 total samples; 33 samples were removed due to low sequencing depth and 34 samples were removed due to sexual differentiation over the course of the exposure.

3.3. Dietary BaP exposure altered composition of gut microbiome

Alpha-diversity indices of gut microbiome decreased with increasing BaP doses. Shannon diversity, which accounts for both evenness and abundance of species present, was marginally different among exposures (Kruskal-Wallis chi-squared = 9.2,

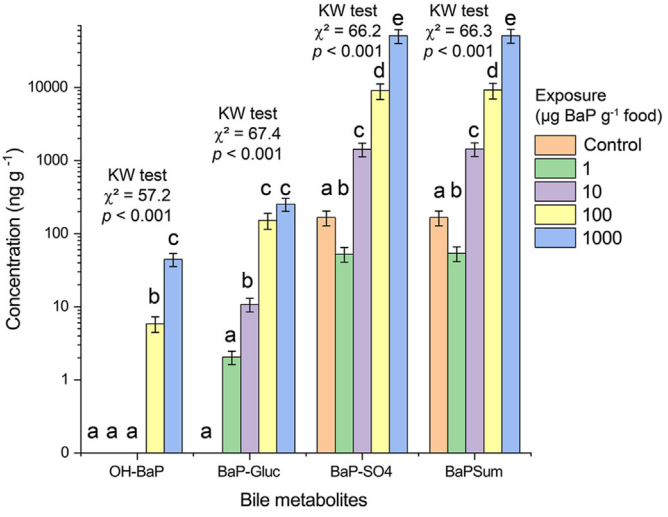

Fig. 1. Concentrations of BaP metabolites (OH–BaP, BaP-Gluc, BaP–SO_4, and the sum of all metabolites) (ng g^{-1}) from bile (±S.E.) on a $\log_{10}$-transformed. Letters denote statistical significance within metabolite groups. KW test, Kruskal–Wallis one-way analysis of variance.

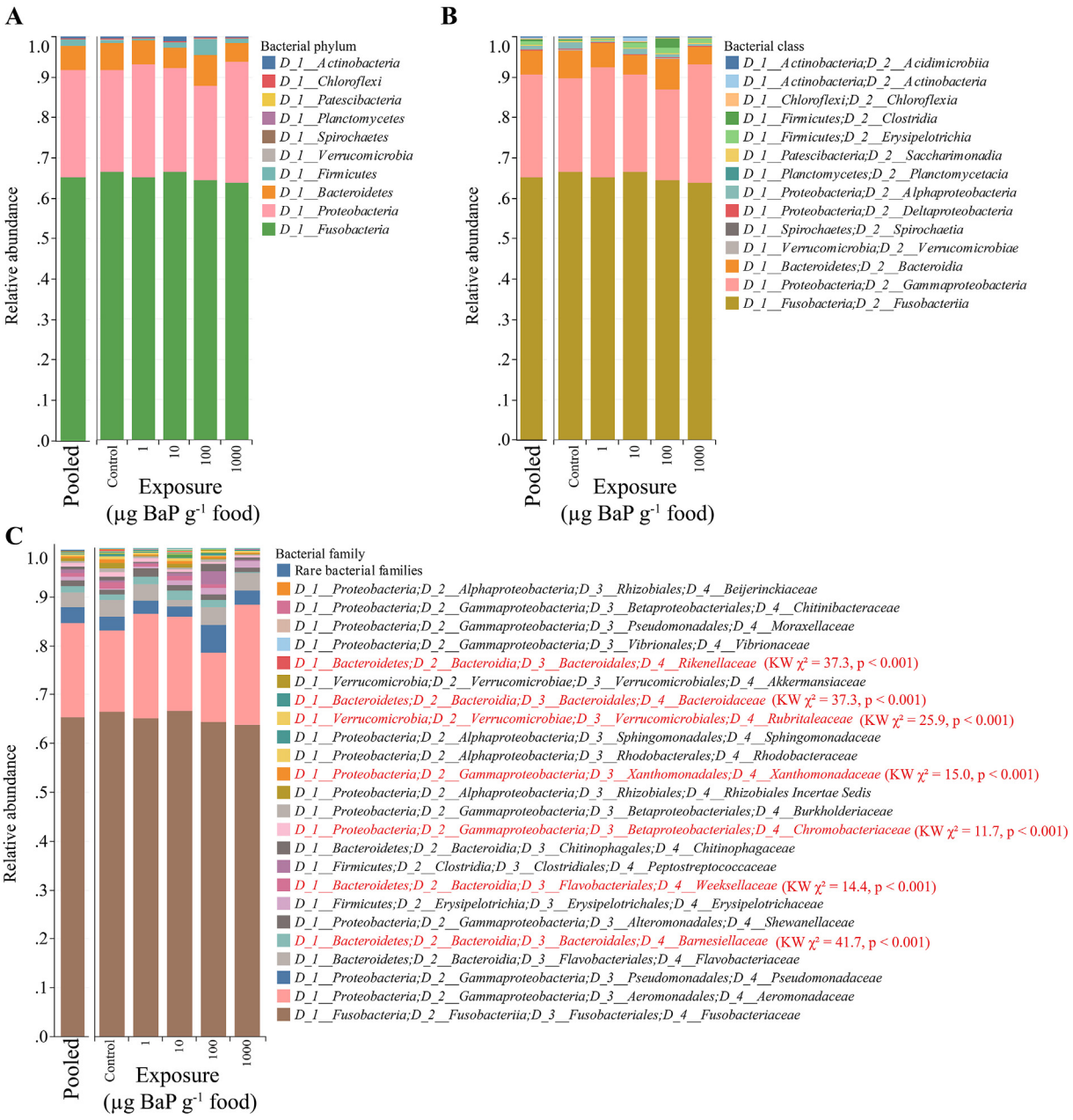

Fig. 2. Relative abundances of more abundant bacterial (A) phyla, (B) class, and (C) families in guts of juvenile fathead minnows, both pooled and based on exposures. KW test, Kruskal–Wallis one-way analysis of variance.

$p = 0.06$), but the Shannon diversity value for the 1000 µg BaP g $^{-1}$ exposure group was significantly less than that of the controls (Dunnett's test, $p = 0.03$; Table 1). Overall, there was an inverse correlation ($r = -0.22$, $p = 0.09$) between Shannon diversity and log_{10}-transformed of concentrations of BaP–SO_4 metabolites (lgBaP-SO_4). The number of observed ASVs was also significantly inversely proportional to exposure concentrations (ANOVA, $F = 8.93$, $p < 0.001$), with the communities in fish fed 1000 µg BaP g $^{-1}$ having significantly fewer ASVs than the control group (Dunnett's test, $p < 0.001$; Table 1). There was also an overall inverse trend between the number of ASVs as a function of log_{10}-transformed concentrations of BaP–SO_4 ($r = -0.36$, $p = 0.004$).

Beta-diversities (unweighted Unifrac distances) of the gut microbiomes were significantly different dependent upon exposure to BaP (Fig. 3A; PERMANOVA test, Pseudo-F = 1.491,

Table 1
Mean values and standard error for Shannon Diversity Index and observed number of amplicon sequence variants (ASVs) for each exposure group. Asterisks denote statistical differences from the control groups, as calculated with Dunnett's tests.

Indices	Exposure (µg g^{-1})	Mean ± S.E
Shannon	Control	4.38 ± 0.13
	1	4.28 ± 0.08
	10	4.43 ± 0.06
	100	4.28 ± 0.18
	1000	4.02 ± 0.12 *
ASVs	Control	91.45 ± 4.75
	1	82.64 ± 4.39
	10	96.5 ± 4.36
	100	86.64 ± 4.4
	1000	62.67 ± 3.11*

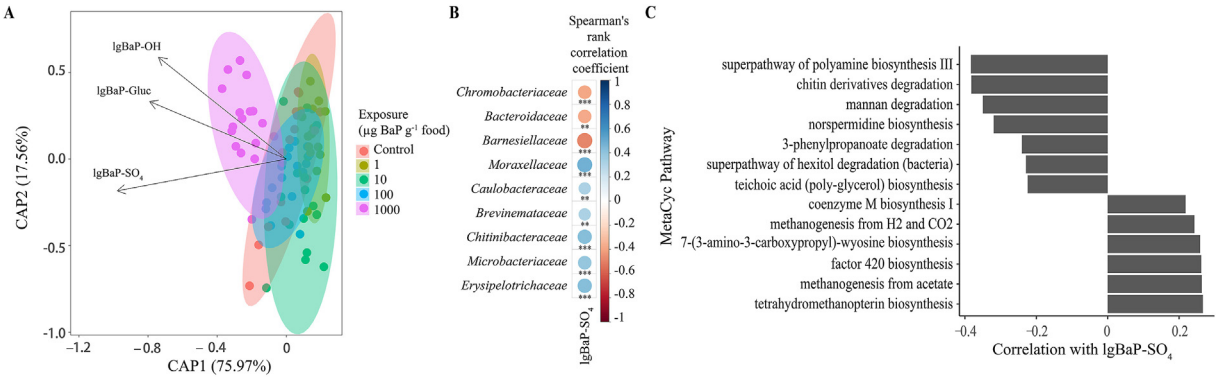

Fig. 3. Responses of the gut microbiome in fathead minnows to dietary exposure of BaP. (A) Constrained Analysis of Principal Coordinates (CAP) of the different exposure groups constrained by the vectors of the measured metabolite concentrations, using unweighted Unifrac distances. lgBaP-OH, log_{10}-transformed of concentrations of OH−BaP metabolite; lgBaP-Gluc, log_{10}-transformed of concentrations of BaP-Gluc metabolite; lgBaP-SO_4, log_{10}-transformed of concentrations of BaP−SO_4 metabolite. (B) Correlation plot of families that are significantly correlated (Spearman correlation, $p < 0.05$) with lgBaP-SO_4. Significance of correlations: ***, $p < 0.001$; **, $p < 0.01$. (C) MetaCyc pathways that are significantly correlated (Spearman correlation, $p < 0.05$) with lgBaP-SO_4. Various pathways are shown relative to their correlation coefficients (ρ).

P_{MC} = 0.047). The 1000 μg BaP g^{-1} exposure group exhibited significantly distinctive unweighted Unifrac distances than that of control, 1, and 10 μg BaP g^{-1} exposure groups (Pairwise PERMANOVA: 1000 μg BaP g^{-1} vs. control, t = 1.529, P_{MC} = 0.024; 1000 μg BaP g^{-1} vs. 1 μg BaP g^{-1}, t = 1.849, P_{MC} = 0.014; 1000 μg BaP g^{-1} vs. 10 μg BaP g^{-1}, t = 1.871, P_{MC} = 0.006). However, weighted Unifrac distances of gut microbiome were not significantly different between groups (PERMANOVA test, Pseudo-F = 1.028, P_{MC} = 0.434), which suggested that BaP did not significantly alter the abundant microbiome. The BaP metabolites used in the dbRDA clustered the exposures in the logical direction of the metabolite vectors, visually indicating that the metabolites were defining the groupings (Fig. 3A). OH−BaP and BaP−SO_4 were significantly constrained the ordination (F = 3.00 and 2.64, p = 0.003 and 0.005, for OH−BaP and BaP−SO_4, respectively).

Exposure to BaP altered families with lesser abundances rather than the dominant bacterial families. Based on exposure groups, several relative abundances of families were significantly different among exposure groups (Fig. 2C). *Barnesiellaceae* (p = 0.03), *Rubritaleaceae* ($p < 0.001$), *Xanthomonadaceae* (p = 0.02), *Weeksellaceae* (p = 0.01), and *Chromobacteriaceae* (p = 0.007) were all significantly less in fish of 1000 μg BaP g^{-1} group relative to the control group. Several relative abundances of families (CLR-transformed) were significantly correlated with lgBaP-SO_4. Relative abundances of families that included *Bacteroidaceae, Barnesiellaceae,* and *Chromobacteriaceae* were significantly negatively correlated with lgBaP-SO_4. While *Brevinemataceae*, *Caulobacteraceae*, *Microbacteriaceae, Erysipelotrichaceae, Chitinibacteraceae,* and *Moraxellacea* significantly positively correlated families with lgBaP-SO_4 (Fig. 3B).

3.4. Dietary BaP exposure altered predicted microbial functional pathways

In total, based on Spearman correlations, 13 inferred MetaCyc pathways were also significantly correlated with lgBaP-SO_4. Seven pathways [superpathway of polyamine biosynthesis III, chitin derivatives degradation, mannan degradation, norspermidine biosynthesis, 3-phenylpropanoate degradation, superpathway of hexitol degradation (bacteria), and teichoic acid (poly-glycerol) biosynthesis] were negatively correlated with lgBaP-SO_4. Six pathways [coenzyme M biosynthesis I, methanogenesis from H2 and CO2, 7-(3-amino-3-carboxypropyl)-wyosine biosynthesis, factor 420 biosynthesis, methanogenesis from acetate, and tetrahydromethanopterin biosynthesis] were positively correlated with concentrations of lgBaP-SO_4 (Fig. 3C).

3.5. Dietary BaP exposure altered association networks of gut microbiome

Dietary exposure to BaP altered the association network of gut microbiomes in fathead minnows. Network structure reveals clusters of microbial associations for each dosage group (Association network at family level, Fig. 4; network at genus level, SI Fig. S3). Network analysis revealed a reduction in the complexity of community structures of gut microbiome in the exposure groups. The major clutters of microbial associations were disrupted in the highest dosage group (Fig. 4E). Number of nodes, heterogeneity, and centralization of treatment groups were less than those of the control group (Table S4).

4. Discussion

The dominant bacterial phyla of gut microbiome in juvenile fathead minnows are consistent with those of other freshwater fishes, which indicates that gut microbiome have conserved biological function among fishes. Dominance of *Fusobacteria* and *Proteobacteria* has been observed not only in other studies utilizing fathead minnows (DeBofsky et al., 2020a; Narrowe et al., 2015), but also in other fish species, such as zebrafish (*Danio rerio*) (Roeselers et al., 2011) and common carp (*Cyprinus carpio*) (Li et al., 2013). Minor differences occurred between the dominant taxa reported in this study and those reported previously for the fathead minnow (DeBofsky et al., 2020a). In this study, *Fusobacteria* was dominant (65%), whereas we previously reported the dominance of *Proteobacteria* (63%). This disparity could have resulted from maturation of these fish, since age or sexual differentiation are driving factors in bacterial community composition (Org et al., 2016; Stephens et al., 2015; Wong et al., 2015).

Patterns between metabolites of BaP and exposure doses measured in this study were also consistent with those found in contaminated sites around the world. Concentrations of biliary metabolites, expressed as BaP equivalents, have been found at concentrations of 193 ng ml^{-1} in *Alepocephalus rostratus*, a deep-sea fish, in the Mediterranean Sea (Escartín and Porte, 1999). Mean sum concentrations of PAH metabolites in bile of lake whitefish (*Coregonus clupeaformis*) in the Athabasca River at Fort McKay in the oil sands region of Canada were 8100 ng ml^{-1}

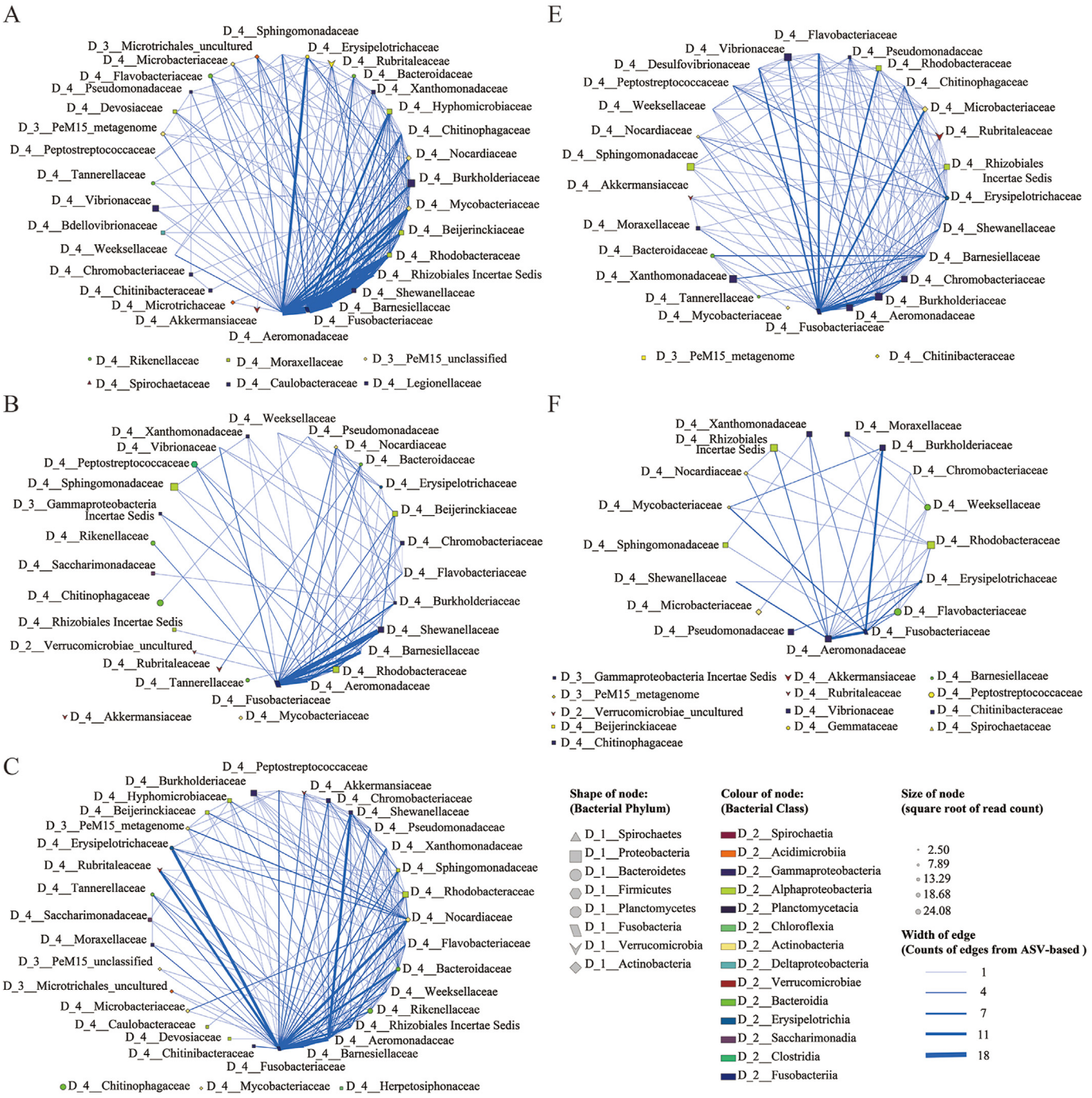

Fig. 4. Association networks of microbial taxa at the class level relative to exposure groups for the (A) control, (B) 1, (C) 10, (D) 100, and (E) 1000 μg BaP g^{-1} exposure groups. Associations were generated by SparCC with 100 bootstraps to assign p-values. The associations were filtered to include only correlations with a correlation $\rho > 0.7$ and a 'two-tailed' p-value < 0.01. Only correlations with $\rho > 0.50$ and $p < 0.05$ (two-tailed) were included. Association networks of microbial ASVs were summarized by ThematicMap App (http://apps.cytoscape.org/apps/thematicmap) at class level. Networks with genus labels are presented in SI Fig. S3.

(Ohiozebau et al., 2016). In this study, mean concentrations of sum BaP metabolites expressed as ng ml^{-1} in bile of fish exposed to 1000 μg BaP g^{-1} was 517 ng ml^{-1}. Therefore, concentrations of BaP fed to fathead minnows resulted in concentrations of metabolites in bile that are in the range of concentrations observed in fishes at moderately contaminated sites. Measuring biliary metabolites reflects recent exposure to PAHs; incorporating concentrations of BaP metabolites into this study allows for comparison to environmental monitoring studies of PAHs, where this is a common practice (Ohiozebau et al., 2016).

The results of this study revealed that a dietary exposure to BaP at environmentally-relevant concentrations have significant effects on the fathead minnow gut microbiome. BaP might be altering the gut microbiome directly or since BaP is a ligand of the aryl hydrocarbon receptor (AhR), via modulation of pathways associated with the AhR (Ortiz-Delgado et al., 2007). The AhR regulates host-microbiome communications (Zhang et al., 2017) in a bidirectional manner (Korecka et al., 2016). Exposure to BaP not only

altered the composition of certain low abundant taxa and overall beta-diversity, but also changed network connectivity of those taxa.

Due to exposure to BaP, there were taxa that were significantly enriched, signifying that certain taxa might be able to use BaP as energy resources. Altered conditions, both in the microbial community and within the host, might allow pathogenic taxa to proliferate (Fig. 3C). The family Caulobacteraceae has been observed in soils contaminated with crude and diesel oils (Bell et al., 2011; Yergeau et al., 2012) and is capable of degradation of aromatic compounds (Nierman et al., 2001). Enrichment of the family Microbacteriaceae has similarly been associated with contaminated soil sites (Bell et al., 2011; Jacques et al., 2007). Increased abundance of the family Er*ysipelotrichaceae* was also observed in mice that were exposed via the diet to BaP (Ribière et al., 2016) and *via* drinking water to heavy metals (Breton et al., 2013). Studies in humans have related abundance of *Erysipelotrichaceae* with colorectal cancer (Chen et al., 2012), a particularly interesting finding since BaP is carcinogenic (Gelboin, 1980). Increases in abundances of bacteria in the family *Moraxellaceae,* which contains several opportunistic pathogens (Austin and Austin, 2016), is associated with increased stress in fish (Boutin et al., 2013). Furthermore, these same taxa are capable of degrading BaP when isolated from human skin (Sowada et al., 2014). Although the taxa were not the same, a similar phenomenon of enrichment of taxa associated with hydrocarbon degradation was seen in (DeBofsky et al, (2020a)).

Analyses of individual taxa also revealed several taxa that were negatively correlated with the BaP−SO4 metabolite that might be associated with direct deleterious effects on the physiology of the host. The presence of the family Bact*eroidaceae* in the gut of a host is considered mutualistic, with both the bacteria and the host benefiting from the interaction (Bäckhed et al., 2005). *Bacteroidaceae* are in part responsible for the production of digestive enzymes and the digestion of polysaccharides (Bäckhed et al., 2005; Ikeda-Ohtsubo et al., 2018; Thomas et al., 2011) and is involved in regulation of the immune system (Hiippala et al., 2018). Mice exposed to 2,3,7,8-tetrachlorodibenzo-*p*-dioxin (TCDD), another AhR modulator, exhibited lesser abundances of several families of Bacteroidetes (Lefever et al., 2016). These results suggest that the reduction in *Bacteroidaceae,* and possibly *Barnesiellaceae*, another member of the order Bacteroidales, might be associated with deleterious effects caused by exposure to BaP, including impairment of immune function (Carlson et al., 2004b; Reynaud and Deschaux, 2006).

Several MetaCyc pathways were significantly associated with concentrations of BaP−SO_4. One pathway, chitin derivatives degradation, which had a negative relationship with BaP−SO_4, is associated with *Bacteroidaceae* (Olsen et al., 1996). Inability to degrade chitin might result in lesser ability to obtain nutrients from food for proper health or defend against pathogens (Ringø et al., 2012). The same holds true for the reduction in the mannan degradation pathway, where reduced ability to degrade mannan might result in increased susceptibility to pathogens (Dimitroglou et al., 2009; Torrecillas et al., 2012), and reduction of teichoic acid (poly-glycerol) biosynthesis, which is involved in activating the innate immune response (Bron et al., 2012; Hoseinifar et al., 2015). Pathways that increased in relation to concentrations of BaP−SO_4 in bile included methanogenesis from H_2 and CO_2 and methanogenesis from acetate. Anaerobic degradation of hydrocarbons to methane and CO_2 requires H_2 and CO_2 utilizing bacteria as well as acetate-utilizing methanogenic bacteria (Chang et al., 2005; Zengler et al., 1999). It is therefore plausible that the exposure results in an enrichment of bacteria capable of degrading hydrocarbons. While these pathways are informative, it should be noted that they are predictive and not confirmed with functional transcriptomic analysis.

The reduction in network complexity was an unexpected result of exposure to BaP. Reduction in the number of nodes represents fewer taxa present in those association networks, while a reduction in the number of edges reflects fewer associations among those nodes (Friedman and Alm, 2012). Although interactions between microbes have not been well-explored (Hunt and Ward, 2015), ecological network responses to anthropogenic perturbation are not new (Elmqvist et al., 2003; Power et al., 1996; Vinebrooke et al., 2004). Loss of co-occurrence of taxa within a microbial community might result in altered interactions among taxa, which can change function of certain taxa or allow proliferation of others (Karimi et al., 2017). At greater concentrations of BaP in the diet, numbers of associations with other taxa decreased, meaning that the abundance of those taxa was independent of other taxa (Karimi et al., 2017). The greater the number of edges, the greater the complexity of the system (Tylianakis et al., 2010), and a large degree of connectedness can be considered a shared ecological niche within the community (Karimi et al., 2017). A reduction in network complexity has been observed in terrestrial systems with high concentrations of air pollution (Karimi et al., 2016) and at a chlor-alkali tailings dump (Zappelini et al., 2015). Losses of nodes, or taxa, and edges, or those connections, signifies the breakdown of the ecological niche. Therefore, loss of community structure in the microbiome could be an indicator of exposure to a toxicant (Derocles et al., 2018).

5. Conclusion

Overall, this study revealed that chronic exposure to BaP in the diet significantly altered the community structure of gut microbiome of juvenile fathead minnows. This work supports previous work (DeBofsky et al., 2020a), which revealed that short-term exposure to very low doses of BaP significantly alters the fathead minnow microbiome. Use of an environmentally-relevant exposure route in a more sensitive life stage provides insight into impacts of BaP on the microbiome before the fish sexually differentiate. The measurement of concentrations of metabolites of BaP in bile was more closely related to effects on individual and community responses and more thoroughly explained diversity than did nominal exposure concentrations in the diet. Several taxa associated with health and hydrocarbon degradation were significantly correlated with measured metabolite concentrations. Community compositions shifted and network associations were drastically altered based on the exposures. These results highlight the need for future work to determine mechanistic causes of community compositional differences and ultimately how gut microbial changes may interplay with host adverse outcomes.

CRediT author statement

Abigail DeBofsky: Investigation, Methodology, Data curation, Writing – original draft. Yuwei Xie: Conceptualization, Methodology, Validation, Writing – review & editing. Jonathan Challis: Resources, Data curation, Writing – review & editing. Niteesh Jain: Resources. Markus Brinkmann: Writing – review & editing. Paul D. Jones: Funding acquisition, Writing – review & editing. John P. Giesy: Conceptualization, Project administration, Funding acquisition, Writing – review & editing.

Declaration of competing interest

The authors declare no competing financial interest.

Acknowledgments

Funding was provided by "Next generation solutions to ensure healthy water resources for future generations" funded by the Global Water Futures program, Canada First Research Excellence Fund (#419205). Dr. Brinkmann was also supported through the Global Water Futures program. Dr. Challis was funded by the Banting Post-Doctoral Fellowship. Prof. Giesy was supported by the Canada Research Chairs Program of the Natural Sciences and Engineering Research Council of Canada (NSERC).

Appendix B. Supplementary data

Supplementary data to this article can be found online at https://doi.org/10.1016/j.envpol.2021.116821.

Appendix ASupporting Information

Text S1, Fish husbandry. Text S2, Quantification of BaP in food. Text S3, Relative quantification of metabolites of BaP in bile. Table S1. Limit of quantification (LOQ) and limit of detection (LOD) of OH−BaP, BaP-Gluc, and BaP−SO4. Table S2. The counts of sequenced, filtered, denoised, merged, non-chimeric, and bacteria only reads for each sample. Table S3. Concentrations of benzo[a] pyrene (BaP) in food and metabolites of BaP in bile. Reported as mean ± standard errors (SE). Table S4. Parameters of co-association gut microbial network. Fig. S1. Rarefaction curve of Shannon Diversity values across sequencing depths. Fig. S2. Condition factor of fish exposed to BaP within each exposure group. Exposure did not significantly affect the condition factors of these fish. Fig. S3. Association networks assembled at the level of genera for (A) Control, (B) 1, (C)10, (D) 100, and (E) 1000 μg BaP g-1. Fig.

References

Adamovsky, O., Buerger, A., Wormington, A.M., Ector, N., Griffitt, R.J., Bisesi, J.H., Martyniuk, C.J., 2018. The gut microbiome and aquatic toxicology: an emerging concept for environmental health. Environ. Toxicol. Chem. 37 (11), 2758−2775. https://doi.org/10.1002/etc.4249.

Austin, B., Austin, D.A., 2016. Bacterial fish pathogens, Disease of Farmed and Wild Fish, Sixth. Springer.

Bäckhed, F., Ley, R.E., Sonnenburg, J.L., Peterson, D.A., Gordon, J.I., 2005. Host-bacterial mutualism in the human intestine. Science 307 (5717), 1915−1920. https://doi.org/10.1126/science.1104816.

Bell, T.H., Yergeau, E., Martineau, C., Juck, D., Whyte, L.G., Greer, C.W., 2011. Identification of nitrogen-incorporating bacteria in petroleum-contaminated arctic soils by using [15N]DNA-based stable isotope probing and pyrosequencing. Appl. Environ. Microbiol. 77, 4163−4171. https://doi.org/10.1128/AEM.00172-11.

Beyer, J., Jonsson, G., Porte, C., Krahn, M.M., Ariese, F., 2010. Analytical methods for determining metabolites of polycyclic aromatic hydrocarbon (PAH) pollutants in fish bile: a review. Environ. Toxicol. Pharmacol. 30, 224−244. https://doi.org/10.1016/j.etap.2010.08.004.

Bolyen, E., Rideout, J.R., Dillon, M.R., Bokulich, N.A., Abnet, C.C., Al-Ghalith, G.A., Alexander, H., Alm, E.J., Arumugam, M., Asnicar, F., Bai, Y., Bisanz, J.E., Bittinger, K., Brejnrod, A., Brislawn, C.J., Brown, C.T., Callahan, B.J., Caraballo-Rodríguez, A.M., Chase, J., Cope, E.K., Da Silva, R., Diener, C., Dorrestein, P.C., Douglas, G.M., Durall, D.M., Duvallet, C., Edwardson, C.F., Ernst, M., Estaki, M., Fouquier, J., Gauglitz, J.M., Gibbons, S.M., Gibson, D.L., Gonzalez, A., Gorlick, K., Guo, J., Hillmann, B., Holmes, S., Holste, H., Huttenhower, C., Huttley, G.A., Janssen, S., Jarmusch, A.K., Jiang, L., Kaehler, B.D., Kang, K. Bin, Keefe, C.R., Keim, P., Kelley, S.T., Knights, D., Koester, I., Kosciolek, T., Kreps, J., Langille, M.G.I., Lee, J., Ley, R., Liu, Y.X., Loftfield, E., Lozupone, C., Maher, M., Marotz, C., Martin, B.D., McDonald, D., McIver, L.J., Melnik, A.V., Metcalf, J.L., Morgan, S.C., Morton, J.T., Naimey, A.T., Navas-Molina, J.A., Nothias, L.F., Orchanian, S.B., Pearson, T., Peoples, S.L., Petras, D., Preuss, M.L., Pruesse, E., Rasmussen, L.B., Rivers, A., Robeson, M.S., Rosenthal, P., Segata, N., Shaffer, M., Shiffer, A., Sinha, R., Song, S.J., Spear, J.R., Swafford, A.D., Thompson, L.R., Torres, P.J., Trinh, P., Tripathi, A., Turnbaugh, P.J., Ul-Hasan, S., van der Hooft, J.J.J., Vargas, F., Vázquez-Baeza, Y., Vogtmann, E., von Hippel, M., Walters, W., Wan, Y., Wang, M., Warren, J., Weber, K.C., Williamson, C.H.D., Willis, A.D., Xu, Z.Z., Zaneveld, J.R., Zhang, Y., Zhu, Q., Knight, R., Caporaso, J.G., Guerrini, C.J., Botkin, J.R., McGuire, A.L., 2019. Reproducible, interactive, scalable and extensible microbiome data science using QIIME 2. Nat. Biotechnol. 37, 850−852. https://doi.org/10.1038/s41587-019-0190-3.

Boutin, S., Bernatchez, L., Audet, C., Derôme, N., 2013. Network Analysis Highlights Complex Interactions between Pathogen, Host and Commensal Microbiota. PLoS One 8 (12), e84772. https://doi.org/10.1371/journal.pone.0084772.

Breton, J., Massart, S., Vandamme, P., De Brandt, E., Pot, B., Foligné, B., 2013. Ecotoxicology inside the gut: impact of heavy metals on the mouse microbiome. BMC Pharmacol. Toxicol. 14, 62. https://doi.org/10.1186/2050-6511-14-62.

Bron, P.A., Van Baarlen, P., Kleerebezem, M., 2012. Emerging molecular insights into the interaction between probiotics and the host intestinal mucosa. Nat. Rev. Microbiol. 21 (10), 66−78. https://doi.org/10.1038/nrmicro2690.

Carding, S., Verbeke, K., Vipond, D.T., Corfe, B.M., Owen, L.J., 2015. Dysbiosis of the gut microbiota in disease. Microb. Ecol. Health Dis. 26, 26191. https://doi.org/10.3402/mehd.v26.26191.

Carlson, E.A., Li, Y., Zelikoff, J.T., 2004a. Suppressive effects of benzo[a]pyrene upon fish immune function: evolutionarily conserved cellular mechanisms of immunotoxicity. Marine Environmental Research, pp. 731−734. https://doi.org/10.1016/j.marenvres.2004.03.023.

Carlson, E.A., Li, Y., Zelikoff, J.T., 2004b. Benzo[a]pyrene-induced immunotoxicity in Japanese medaka (Oryzias latipes): relationship between lymphoid CYP1A activity and humoral immune suppression. Toxicol. Appl. Pharmacol. 201, 40−52. https://doi.org/10.1016/j.taap.2004.04.018.

Caspi, R., Billington, R., Fulcher, C.A., Keseler, I.M., Kothari, A., Krummenacker, M., Latendresse, M., Midford, P.E., Ong, Q., Ong, W.K., Paley, S., Subhraveti, P., Karp, P.D., 2017. The MetaCyc database of metabolic pathways and enzymes. Nucleic Acids Res. 46, 633−639. https://doi.org/10.1093/nar/gkx935.

Chang, W., Um, Y., Hoffman, B., Pulliam Holoman, T.R., Holoman, T.R.P., 2005. Molecular characterization of polycyclic aromatic hydrocarbon (PAH)-degrading methanogenic communities. Biotechnol. Prog. 21, 682−688. https://doi.org/10.1021/bp049579l.

Chen, W., Liu, F., Ling, Z., Tong, X., Xiang, C., 2012. Human intestinal lumen and mucosa-associated microbiota in patients with colorectal cancer. PloS One 7. https://doi.org/10.1371/journal.pone.0039743.

Claisse, D., 1989. Chemical contamination of French coasts. Mar. Pollut. Bull. 20, 523−528.

Costa, J., Ferreira, M., Rey-Salgueiro, L., Reis-Henriques, M.A., 2011. Comparision of the waterborne and dietary routes of exposure on the effects of Benzo(a)pyrene on biotransformation pathways in Nile tilapia (Oreochromis niloticus). Chemosphere 84, 1452−1460. https://doi.org/10.1016/j.chemosphere.2011.04.046.

DeBofsky, A., Xie, Y., Grimard, C., Alcaraz, A.J., Brinkmann, M., Hecker, M., Giesy, J.P., 2020. Differential responses of gut microbiota of male and female fathead minnow (Pimephales promelas) to a short-term environmentally-relevant, aqueous exposure to benzo[a]pyrene. Chemosphere 252, 126461. https://doi.org/10.1016/j.chemosphere.2020.126461.

DeBofsky, A., Xie, Y., Jardine, T.D., Hill, J.E., Jones, P.D., Giesy, J.P., 2020b. Effects of the husky oil spill on gut microbiota of native fishes in the North Saskatchewan River, Canada. Aquat. Toxicol. 229 https://doi.org/10.1016/j.aquatox.2020.105658.

Derocles, S.A.P., Bohan, D.A., Dumbrell, A.J., Kitson, J.J., Massol, F., Pauvert, C., Plantegenest, M., Vacher, C., Evans, D.M., 2018. Biomonitoring for the 21st century: integrating next-generation sequencing into ecological network analysis. Advances in Ecological Research, pp. 1−62. https://doi.org/10.1016/bs.aecr.2017.12.001.

Dimitroglou, A., Merrifield, D.L., Carnevali, O., Picchietti, S., Avella, M., Daniels, C., Güroy, D., Davies, S.J., 2011. Microbial manipulations to improve fish health and production − A Mediterranean perspective. Fish Shellfish Immunol. 30 (1), 1−16. https://doi.org/10.1016/j.fsi.2010.08.009.

Dimitroglou, A., Merrifield, D.L., Moate, R., Davies, S.J., Spring, P., Sweetman, J., Bradley, G., 2009. Dietary mannan oligosaccharide supplementation modulates intestinal microbial ecology and improves gut morphology of rainbow trout, Oncorhynchus mykiss (Walbaum). J. Anim. Sci. 87, 3226−3234. https://doi.org/10.2527/jas.2008-1428.

Douglas, G.M., Maffei, V.J., Zaneveld, J., Yurgel, S.N., Brown, J.R., Taylor, C.M., Huttenhower, C., Langille, M.G.I., 2019. PICRUSt2: an Improved and Extensible Approach for Metagenome Inference. bioRxiv 672295. https://doi.org/10.1101/672295.

Elmqvist, T., Folke, C., Nyström, M., Peterson, G., Bengtsson, J., Walker, B., Norberg, J., 2003. Response diversity, ecosystem change, and resilience. Front. Ecol. Environ. 1, 488−494. https://doi.org/10.1890/1540-9295(2003)001[0488:RDECAR]2.0.CO;2.

Escartín, E., Porte, C., 1999. Hydroxylated PAHs in bile of deep-sea fish. Relationship with xenobiotic metabolizing enzymes. Environ. Sci. Technol. 33, 2710−2714. https://doi.org/10.1021/es9902322.

Fernandes, A.D., Reid, J.NS., Macklaim, J.M., McMurrough, T.A., Edgell, D.R., Gloor, G.B., 2014. Unifying the analysis of high-throughput sequencing datasets: characterizing RNA-seq, 16S rRNA gene sequencing and selective growth experiments by compositional data analysis. Microbiome 2, 15. https://doi.org/10.1186/2049-2618-2-15.

Friedman, J., Alm, E.J., 2012. Inferring correlation networks from genomic survey data. PLoS Comput. Biol. 8, 1002687. https://doi.org/10.1371/journal.pcbi.1002687.

Gelboin, H.V., 1980. Benzo[alpha]pyrene metabolism, activation and carcinogenesis: role and regulation of mixed-function oxidases and related enzymes. Physiol. Rev. 60 (4), 1107−1166. https://doi.org/10.1152/physrev.1980.60.4.1107.

He, X., Qi, Z., Hou, H., Qian, L., Gao, J., Zhang, X.X., 2019. Structural and functional alterations of gut microbiome in mice induced by chronic cadmium exposure. Chemosphere 246, 125747. https://doi.org/10.1016/j.chemosphere.2019.125747.

Hiippala, K., Jouhten, H., Ronkainen, A., Hartikainen, A., Kainulainen, V., Jalanka, J., Satokari, R., 2018. The potential of gut commensals in reinforcing intestinal barrier function and alleviating inflammation. Nutrients 10 (8), 988. https://doi.org/10.3390/nu10080988.

Hoseinifar, S.H., Esteban, M.Á., Cuesta, A., Sun, Y., Hossein Hoseinifar, S., Ángeles Esteban, M., Cuesta, A., Sun, Y., Angeles Esteban, M., Sun, Y., 2015. Prebiotics and fish immune response: a review of current knowledge and future perspectives. Rev. Fish. Sci. Aquac. 23, 315–328. https://doi.org/10.1080/23308249.2015.1052365.

Hunt, D.E., Ward, C.S., 2015. A network-based approach to disturbance transmission through microbial interactions. Front. Microbiol. 6, 1182. https://doi.org/10.3389/fmicb.2015.01182.

Ikeda-Ohtsubo, W., Brugman, S., Warden, C.H., Rebel, J.M.J., Folkerts, G., Pieterse, C.M.J., 2018. How can we define "optimal microbiota?": a comparative review of structure and functions of microbiota of animals, fish, and plants in agriculture. Front. Nutr. 5 (90), 1–18. https://doi.org/10.3389/fnut.2018.00090.

Jacques, R.J.S., Okeke, B.C., Bento, F.M., Peralba, M.C.R., Camargo, F.A.O., 2007. Characterization of a polycyclic aromatic hydrocarbon-degrading microbial consortium from a petrochemical sludge landfarming site. Ann. Finance 11, 1–11. https://doi.org/10.1080/10889860601185822.

Karimi, B., Maron, P.A., Chemidlin-Prevost Boure, N., Bernard, N., Gilbert, D., Ranjard, L., 2017. Microbial diversity and ecological networks as indicators of environmental quality. Environ. Chem. Lett. 15, 265–281. https://doi.org/10.1007/s10311-017-0614-6.

Karimi, B., Meyer, C., Gilbert, D., Bernard, N., 2016. Air pollution below WHO levels decreases by 40 % the links of terrestrial microbial networks. Environ. Chem. Lett. 14, 467–475. https://doi.org/10.1007/s10311-016-0589-8.

Knutzen, J., Sortland, B., 1982. Polycyclic aromatic hydrocarbons (PAH) in some algae and invertebrates from moderately polluted parts of the coast of Norway. Water Res. 16, 421–428. https://doi.org/10.1016/0043-1354(82)90166-X.

Korecka, A., Dona, A., Lahiri, S., Tett, A.J., Al-Asmakh, M., Braniste, V., D'Arienzo, R., Abbaspour, A., Reichardt, N., Fujii-Kuriyama, Y., Rafter, J., Narbad, A., Holmes, E., Nicholson, J., Arulampalam, V., Pettersson, S., 2016. Bidirectional communication between the Aryl hydrocarbon Receptor (AhR) and the microbiome tunes host metabolism. npj Biofilms Microbiomes 2, 16014. https://doi.org/10.1038/npjbiofilms.2016.14.

Lefever, D.E., Xu, J., Chen, Y., Huang, G., Tamas, N., Guo, T.L., 2016. TCDD modulation of gut microbiome correlated with liver and immune toxicity in streptozotocin (STZ)-induced hyperglycemic mice. Toxicol. Appl. Pharmacol. 304, 48–58. https://doi.org/10.1016/j.taap.2016.05.016.

Li, X., Yan, Q., Xie, S., Hu, W., Yu, Y., 2013. Gut microbiota contributes to the growth of fast-growing transgenic common carp (Cyprinus carpio L.). PloS One 8, 64577. https://doi.org/10.1371/journal.pone.0064577.

Llewellyn, M.S., Boutin, S., Hoseinifar, S.H., Derome, N., 2014. Teleost microbiomes: the state of the art in their characterization, manipulation and importance in aquaculture and fisheries. Front. Microbiol. 5, 207. https://doi.org/10.3389/fmicb.2014.00207.

Lozupone, C., Knight, R., 2005. UniFrac: a new phylogenetic method for comparing microbial communities. Appl. Environ. Microbiol. 71, 8228–8235. https://doi.org/10.1128/AEM.71.12.8228-8235.2005.

Malins, D.C., McCain, B.B., Brown, D.W., Varanasi, U., Krahn, M.M., Myers, M.S., Chan, S.L., 1987. Sediment-associated contaminants and liver diseases in bottom-dwelling fish. Hydrobiologia 149, 67–74. https://doi.org/10.1007/BF00048647.

Mccarthy, J.F., Burrus, L.W., Tolbert, V.R., 2003. Bioaccumulation of benzo(a)pyrene from sediment by fathead minnows: effects of organic content, resuspension and metabolism environmental contamination a n d toxicology. Arch. Environ. Contam. Toxicol. 45, 364–370. https://doi.org/10.1007/s00244-003-2148-0.

Nacci, D.E., Kohan, M., Pelletier, M., George, E., 2002. Effects of benzo[a]pyrene exposure on a fish population resistant to the toxic effects of dioxin-like compounds. Aquat. Toxicol. 57 (4), 203–215.

Narrowe, A.B., Albuthi-Lantz, M., Smith, E.P., Bower, K.J., Roane, T.M., Vajda, A.M., Miller, C.S., 2015. Perturbation and restoration of the fathead minnow gut microbiome after low-level triclosan exposure. Microbiome 3, 6. https://doi.org/10.1186/s40168-015-0069-6.

Neff, J.M., Stout, S.A., Gunster, D.G., 2005. Ecological risk assessment of polycyclic aromatic hydrocarbons in sediments: identifying sources and ecological hazard. Integrated Environ. Assess. Manag. 1, 22–33. https://doi.org/10.1897/IEAM_2004a-016.1.

Nichols, J.W., McKim, J.M., Lien, G.J., Hoffman, A.D., Bertelsen, S.L., Elonen, C.M., 1996. A physiologically based toxicokinetic model for dermal absorption of organic chemicals by fish. Fund. Appl. Toxicol. 31, 229–242. https://doi.org/10.1006/faat.1996.0095.

Nierman, W.C., Feldblyum, T.V., Laub, M.T., Paulsen, I.T., Nelson, K.E., Eisen, J., Heidelberg, J.F., Alley, M.R.K., Ohta, N., Maddock, J.R., Potocka, I., Nelson, W.C., Newton, A., Stephens, C., Phadke, N.D., Ely, B., DeBoy, R.T., Dodson, R.J., Durkin, A.S., Gwinn, M.L., Haft, D.H., Kolonay, J.F., Smit, J., Craven, M.B., Khouri, H., Shetty, J., Berry, K., Utterback, T., Tran, K., Wolf, A., Vamathevan, J., Ermolaeva, M., White, O., Salzberg, S.L., Venter, J.C., Shapiro, L., Fraser, C.M., 2001. Complete genome sequence of Caulobacter crescentus. Proc. Natl. Acad. Sci. U. S. A 98, 4136–4141. https://doi.org/10.1073/pnas.061029298.

Nishimoto, M., Yanagida, G.K., Stein, J.E., Baird, W.M., Varanasi, U., 1992. The metabolism of benzo(a)pyrene by English sole (parophrys vetulus): comparison between isolated hepatocytes in vitro and liver in vivo. Xenobiotica 22, 949–961. https://doi.org/10.3109/00498259209049901.

Ohiozebau, E., Tendler, B., Hill, A., Codling, G., Kelly, E., Giesy, J.P., Jones, P.D., 2016. Products of biotransformation of polycyclic aromatic hydrocarbons in fishes of the Athabasca/Slave river system, Canada. Environ. Geochem. Health 38, 577–591. https://doi.org/10.1007/s10653-015-9744-6.

Oksanen, J., Blanchet, F.G., Friendly, M., Kindt, R., Legendre, P., McGlinn, D., Minchin, P.R., O'Hara, R.B., Simpson, G.L., Solymos, P., Stevens, M.H.H., Szoecs, E., Wagner, H., 2019. Vegan: community ecology package.

Olsen, M.A., Aagnes, T.H., Sørmo, W., Mathiesen, S.D., 1996. Chitinolytic bacteria in the minke whale forestomach. Anim. Res. 45, 287. https://doi.org/10.1139/w99-112.

Org, E., Mehrabian, M., Parks, B.W., Shipkova, P., Liu, X., Drake, T.A., Lusis, A.J., 2016. Sex differences and hormonal effects on gut microbiota composition in mice. Gut Microb. 7, 313–322. https://doi.org/10.1080/19490976.2016.1203502.

Ortiz-Delgado, J.B., Segner, H., Arellano, J.M., Sarasquete, C., 2007. Histopathological alterations, EROD activity, CYP1A protein and biliary metabolites in gilthead seabream Sparus aurata exposed to Benzo(a)pyrene. Histol. Histopathol. 22, 417–432. https://doi.org/10.14670/HH-22.417.

Pérez, T., Balcázar, J.L., Ruiz-Zarzuela, I., Halaihel, N., Vendrell, D., De Blas, I., Múzquiz, J.L., Múezquiz, J.L., 2010. Host–microbiota interactions within the fish intestinal ecosystem. Mucosal Immunol. 3, 355–360. https://doi.org/10.1038/mi.2010.12.

Phalen, L.J., Köllner, B., Leclair, L.A., Hogan, N.S., Van Den Heuvel, M.R., 2014. The effects of benzo[a]pyrene on leucocyte distribution and antibody response in rainbow trout (Oncorhynchus mykiss). Aquat. Toxicol. 147, 121–128. https://doi.org/10.1016/j.aquatox.2013.12.017.

Power, M.E., Tilman, D., Estes, J.A., Menge, B.A., Bond, W.J., Mills, L.S., Daily, G., Castilla, J.C., Lubchenco, J., Paine, R.T., 1996. Challenges in the quest for keystones. Bioscience 46, 609–620. https://doi.org/10.2307/1312990.

R Core Team, 2013. R: A Language and Environment for Statistical Computing.

Raghunathan, T.E., 2004. What do we do with missing data? Some options for analysis of incomplete data. Annu. Rev. Publ. Health 25, 99–117. https://doi.org/10.1146/annurev.publhealth.25.102802.124410.

Reynaud, S., Deschaux, P., 2006. The Effects of Polycyclic Aromatic Hydrocarbons on the Immune System of Fish: A Review. Aquat. Toxicol. 77 (2), 229–238. https://doi.org/10.1016/j.aquatox.2005.10.018.

Ribière, C., Peyret, P., Parisot, N., Darcha, C., Déchelotte, P.J., Barnich, N., Peyretaillade, E., Boucher, D., 2016. Oral exposure to environmental pollutant benzo[a]pyrene impacts the intestinal epithelium and induces gut microbial shifts in murine model. Sci. Rep. 6, 1–11. https://doi.org/10.1038/srep31027.

Ringø, E., Zhou, Z., Olsen, R.E., Song, S.K., 2012. Use of chitin and krill in aquaculture - the effect on gut microbiota and the immune system: a review. Aquacult. Nutr. 18, 117–131. https://doi.org/10.1111/j.1365-2095.2011.00919.x.

Roeselers, G., Mittge, E.K., Stephens, W.Z., Parichy, D.M., Cavanaugh, C.M., Guillemin, K., Rawls, J.F., 2011. Evidence for a core gut microbiota in the zebrafish. ISME J. 5, 1595–1608. https://doi.org/10.1038/ismej.2011.38.

Rolig, A.S., Parthasarathy, R., Burns, A.R., Bohannan, B.J.M.M., Guillemin, K., Correspondence, K.G., Guillemin, K., Correspondence, K.G., Guillemin, K., Correspondence, K.G., Guillemin, K., 2015. Individual members of the microbiota disproportionately modulate host innate immune responses. Cell Host Microbe 18, 613–620. https://doi.org/10.1016/j.chom.2015.10.009.

Salinas, I., Magadán, S., 2017. Omics in fish mucosal immunity. Dev. Comp. Immunol. 75, 99–108. https://doi.org/10.1016/j.dci.2017.02.010.

Sandvik, M., Horsberg, T.E., Skaare, J.U., Ingebrigtsen, K., 1998. Comparison of dietary and waterborne exposure to benzo[a]pyrene: bioavailability, tissue disposition and CYP1A1 induction in rainbow trout (Oncorhynchus mykiss). Biomarkers 3, 399–410. https://doi.org/10.1080/135475098231048.

Schlenk, D., Celander, M., Gallagher, E.P., George, S., James, M., Kullman, S.W., 2008. Biotransformation in fishes. In: DI Giulio, R., Hinton, D.E. (Eds.), The Toxicology of Fishes. CRC Press, Taylor and Francis Group, London, pp. 153–234.

Shannon, P., Markiel, A., Ozier, O., Baliga, N.S., Wang, J.T., Ramage, D., Amin, N., Schwikowski, B., Ideker, T., 2003. Cytoscape: a software Environment for integrated models of biomolecular interaction networks. Genome Res. 13, 2498–2504. https://doi.org/10.1101/gr.1239303.

Silva, A.C.F., Hawkins, S.J., Boaventura, D.M., Thompson, R.C., 2008. Predation by small mobile aquatic predators regulates populations of the intertidal limpet Patella vulgata (L.). J. Exp. Mar. Biol. Ecol. 367, 259–265. https://doi.org/10.1016/j.jembe.2008.10.010.

Snyder, S.M., Pulster, E.L., Wetzel, D.L., Murawski, S.A., 2015. PAH exposure in gulf of Mexico demersal fishes, post- deepwater horizon. Environ. Sci. Technol. 49, 8786–8795. https://doi.org/10.1021/acs.est.5b01870.

Sowada, J., Schmalenberger, A., Ebner, I., Luch, A., Tralau, T., 2014. Degradation of benzo[a]pyrene by bacterial isolates from human skin. FEMS Microbiol. Ecol. 88, 129–139. https://doi.org/10.1111/1574-6941.12276.

Srogi, K., 2007. Monitoring of environmental exposure to polycyclic aromatic hydrocarbons: a review. Environ. Chem. Lett. 5 (4), 169–195. https://doi.org/10.1007/s10311-007-0095-0.

Stephens, Z.W., Burns, A.R., Stagaman, K., Wong, S., Rawls, J.F., Guillemin, K., Bohannan, B.J.M., 2015. The composition of the zebrafish intestinal microbial community varies across development. ISME J. 10, 1–11. https://doi.org/10.1038/ismej.2015.140.

Thomas, F., Hehemann, J.H., Rebuffet, E., Czjzek, M., Michel, G., 2011. Environmental and gut Bacteroidetes: the food connection. Front. Microbiol. 2 https://doi.org/10.3389/fmicb.2011.00093.

Torrecillas, S., Makol, A., Caballero, M.J., Montero, D., Dhanasiri, A.K.S., Sweetman, J., Izquierdo, M., 2012. Effects on mortality and stress response in European sea

bass, Dicentrarchus labrax (L.), fed mannan oligosaccharides (MOS) after Vibrio anguillarum exposure. J. Fish. Dis. 35, 591–602. https://doi.org/10.1111/j.1365-2761.2012.01384.x.

Tuvikene, A., 1995. Responses of fish to polycyclic aromatic hydrocarbons (PAHs). Ann. Zool. Fenn. 32, 295–309. https://doi.org/10.2307/23735700.

Tylianakis, J.M., Laliberté, E., Nielsen, A., Bascompte, J., 2010. Conservation of species interaction networks. Biol. Conserv. 143 (10), 2270–2279. https://doi.org/10.1016/j.biocon.2009.12.004.

Vinebrooke, R.D., Cottingham, K.L., Norberg, J., Scheffer, M., Dodson, S.I., Maberly, S.C., Sommer, U., 2004. Impacts of multiple stressors on biodiversity and ecosystem functioning: the role of species co-tolerance. Oikos 104, 451–457. https://doi.org/10.1111/j.0030-1299.2004.13255.x.

Wang, X., Wang, W.-X., 2006. Bioaccumulation and transfer of benzo(a)pyrene in a simplified marine food chain. Mar. Ecol. Prog. Ser. 312, 101–111. https://doi.org/10.1017/CBO9781107415324.004.

Wong, S., Zac Stephens, W., Burns, A.R., Stagaman, K., David, L.A., Bohannan, B.J.M., Guillemin, K., Rawls, J.F., 2015. Ontogenetic differences in dietary fat influence microbiota assembly in the zebrafish gut. mBio 6, 1–9. https://doi.org/10.1128/mBio.00687-15.

Yergeau, E., Sanschagrin, S., Beaumier, D., Greer, C.W., 2012. Metagenomic analysis of the bioremediation of diesel-contaminated Canadian high arctic soils. PloS One 7, 30058. https://doi.org/10.1371/journal.pone.0030058.

Zappelini, C., Karimi, B., Foulon, J., Lacercat-Didier, L., Maillard, F., Valot, B., Blaudez, D., Cazaux, D., Gilbert, D., Yergeau, E., Greer, C., Chalot, M., 2015. Diversity and complexity of microbial communities from a chlor-alkali tailings dump. Soil Biol. Biochem 90, 101–110. https://doi.org/10.1016/j.soilbio.2015.08.008.

Zengler, K., Richnow, H.H., Rosselló-Mora, R., Michaelis, W., Widdel, F., 1999. Methane formation from long-chain alkanes by anaerobic microorganisms. Nature 401, 266–269. https://doi.org/10.1038/45777.

Zhang, L., Nichols, R.G., Patterson, A.D., 2017. The aryl hydrocarbon receptor as a moderator of host-microbiota communication. Curr. Opin. Toxicol. 2, 30–35. https://doi.org/10.1016/j.cotox.2017.02.001.

Zhao, Y., Liu, H., Wang, Q., Li, B., Zhang, H., Pi, Y., 2019. The effects of benzo[a]pyrene on the composition of gut microbiota and the gut health of the juvenile sea cucumber Apostichopus japonicus Selenka. Fish Shellfish Immunol. 93, 369–379.

Supporting information for

Responses of juvenile fathead minnow (*Pimephales promelas*) gut microbiome to a chronic dietary exposure of benzo[*a*]pyrene

Abigail DeBofsky[†], Yuwei Xie[†*], Jonathan Challis[†], Niteesh Jain[†], Markus Brinkmann[†,‡,#], Paul D. Jones[†‡], John P. Giesy[†,§,¥]

[†]Toxicology Centre, University of Saskatchewan, Saskatoon, Saskatchewan, Canada
[‡]School of Environment and Sustainability, University of Saskatchewan, Saskatoon, Saskatchewan, Canada
[#]Global Institute for Water Security, University of Saskatchewan, Saskatoon, Saskatchewan, Canada
[§]Department of Veterinary Biomedical Sciences, University of Saskatchewan, Saskatoon, Saskatchewan, Canada
[¥]Department of Environmental Science, Baylor University, Waco, Texas, USA

* Corresponding author at Toxicology Centre, University of Saskatchewan, Saskatoon, S7N 5B3, Saskatchewan, Canada. Tel: +01-306-9664978

E-mail address: yuwei.xie@usask.ca (YW Xie)

MATERIALS AND METHODS

Text S1, Fish husbandry. Juvenile fathead minnows were obtained from an in-house stock population of the Aquatic Toxicology Research Facility at the University of Saskatchewan. Fish were acclimated at a density of ten juvenile fish per 5-gallon tank containing pretreated facility water, and approximately two-thirds of the water was siphoned and renewed daily. To maintain a temperature of 25 ± 1 °C, tanks were placed in a water bath containing electric heaters. A 16h-light:8h-dark photoperiod was provided. Fish were fed EWOS® Micro Crumble trout chow (Cargill Inc., Wayzata, MN), two times daily on a maintenance food ration (2% of their average wet body mass (bm) per day).

Text S2, Quantification of BaP in food. To quantify BaP in food, stock solutions of BaP and deuterium labelled BaP-d12 were made at 1,000 µg mL^{-1} in acetone. Internal calibration and isotope dilution were used to quantify BaP in samples using an eight-point calibration curve between 0.5 and 500 ng BaP mL^{-1}, each containing 100 ng mL^{-1} with BaP-d12. Isotope dilution was used to confirm concentrations of BaP spiked in fish feed used for the dietary exposure. Triplicate samples of feed (control, 1, 10, 100, 1,000 ug g^{-1} nominal concentrations) were weighed (0.05 g) and spiked with BaP-d12 at a target concentration of 100 ng/mL in the final 1 mL extract. Each sample was loaded into an 11-mL accelerated solvent extraction (ASE) cell as follows: filter paper, 8 g Ottawa Sand (Fisher Scientific), filter paper, fish food sample, filter paper, sand to top of cell, filter paper. Pressurized liquid extraction was conducted using a Dionex ASE 200 with a 1:1 dichloromethane: acetone solvent mixture. Two 70% volume extractions were conducted at 100 ºC and 1,500 psi for 10 min each. A blank cell (no fish food) was also loaded and extracted to serve as an extraction blank. The resulting ≈15 mL extracts

were either blown-down by nitrogen evaporation or diluted and subsampled in order to maintain concentrations within the linear dynamic range of the calibration curve.

Quantification of BaP was done by GC-QE-Orbitrap mass spectrometer system (Q Exactive GC, Thermo Scientific, Mississauga, ON) with a Thermo RSH autosampler and a TRACE 1310 GC with a heated split/splitless injector running in splitless mode. Ionization was by electron impact (EI) ionization at 70 eV. Helium was the carrier gas at a constant flow of 1.0 mL/min. GC separation was achieved on a 60-m DB5ms column (0.1 mm ID, 0.1 μm film thickness) with the following temperature program: 80 ºC (5 min hold), ramping at 4 ºC/min to 325 ºC for a total runtime of 76 min. The instrument was operated at a nominal mass resolution of 120,000 (FWHM) in full scan MS mode (100-425 m/z). Data were acquired and processed in Xcalibur 4.1 (Thermo Scientific, Mississauga, ON).

Text S3, Relative quantification of metabolites of BaP in bile. Bile samples were first weighed, then diluted 1:10 in acetonitrile before analysis. Stock solutions of mono-hydroxyalated benzo[a]pyrene (OH-BaP) (Toronto Research Chemicals, North York, Canada) were made in HPLC grade methanol/ACN (Fisher Scientific). A six point OH-BaP calibration curve ranging from 0.3 – 100 μg L^{-1} was used for semi-quantification of the all BaP metabolites. Analysis was conducted using a Vanquish UHPLC and Q-Exactive™ HF Quadrupole-Orbitrap™ mass spectrometer (Thermo-Fisher). LC separation was achieved with an Acclaim Vanquish 2.2μm C18 LC column (150 x 2.1 mm) (Thermo-Fisher) using a gradient elution with water and acetonitrile, both containing 0.1% formic acid at a flow rate of 0.25 mL/min and column temperature of 30 ºC. The gradient started and was held at 25% ACN from 0-3 min, ramped from 25% to 100% ACN from 3-15 min, held at 100% ACN from 15-18 min, and re-equilibrated to 25% ACN over 7 min for a total run time of 25 min. Retention times of OH-BaP,

OH-BaP-O-glucuronide (BaP-Gluc), and sulfate-BaP (BaP-SO_4) were 12.74, 8.39, and 10.82 minutes, respectively.

Samples were ionized by negative mode heated electrospray ionization (HESI) with the following source parameters: sheath gas flow = 35; aux gas flow = 8; sweep gas flow = 1; aux gas heater = 325ºC; spray voltage = 2.7 kV; S-lens RF = 55; capillary temperature = 300ºC. A Full MS/parallel reaction monitoring (PRM) method was used with the following scan settings: 60,000/30,000 resolution, AGC target = $1x10^6/2x10^5$, max injection time = 100ms/100ms, full MS scan range of 80-500 m/z and PRM isolation window of 2.0 m/z and normalized collision energy = 30. The method monitored the $[M-H]^-$ parent ion m/z 267.080 for OH-BaP and both parent and daughter ions for OH-BaP-O-glucuronide (m/z 443.113 → 267.080) and BaP-SO_4 (m/z 347.038 → 267.080).

Concentrations of OH-BaP were quantified directly with the use of analytical standards and external calibration. Semi-quantification of BaP-Gluc and BaP-SO_4 was conducted using a relative response factor approach. First, a representative set of bile samples were analyzed untreated, followed by analysis of samples treated with glucuronidase and arylsulfatase (30/60 U mL^{-1}; Sigma Aldrich Roche, Basel, Switzerland) in order to convert all of the BaP-Gluc and BaP-SO_4 metabolites present in the untreated samples into OH-BaP. Sample incubations with enzymes were conducted by placing the bile with the enzymes in an incubator for 2 hours at 37°C while shaking at 200 rpm.

These samples provided an instrument response factor for semi-quantification. The response factors for BaP-Gluc and BaP-SO_4 were calculated (Equation 1).

$$Response\ factor = \frac{Peak\ Area\ [OH-BaP]_{treated}}{Peak\ Area\ [Gluc/SO4-BaP]_{untreated}}$$

Mean response factor for Gluc and SO_4 was 21 and 17 respectively, suggesting that for equimolar amounts of OH and Gluc/SO_4 BaP, OH-BaP response was 21 and 17 times more sensitive, respectively. Response factors were used to convert peak areas of OH-BaP from the standard curve to Gluc and SO_4 BaP peak areas in order to construct external calibration curves for each metabolite. Concentrations of each metabolite measured in the extracted bile samples could then be determined from the peak areas. Final BaP metabolite concentrations were reported as ng g^{-1} bile calculated from the volume of solvent used for extraction and specific bile weight.

95 Table S1. Limit of quantification (LOQ) and limit of detection (LOD) of OH-BaP, BaP-Gluc,

96 and BaP-SO_4.

97

Metabolite	LOQ (ng ml^{-1})	LOD (ng ml^{-1})
OH-BaP	0.036	0.011
BaP-Gluc	0.76	0.23
BaP-SO_4	0.61	0.19

98

99 Table S2. The counts of sequenced, filtered, denoised, merged, non-chimeric, and bacteria only

100 reads for each sample

sample	sequenced	filtered	denoised	merged	non-chimeric	bacteria only
NTC2D	593	583	526	429	384	378
NTCD	8	8	2	2	2	2
R11000F2D	24528	24210	23414	21156	16394	16388
R11000F2xD	46308	45695	45155	43248	37550	36568
R11000F3D	21345	21023	20623	19381	16013	16009
R11000F4D	47	36	24	21	21	21
R11000F5D	30502	30114	29740	28581	23489	23400
R11000F6D	30042	29646	29157	27573	22953	22953
R11000F7D	27175	26796	26380	25064	19623	19580
R11000F8D	18001	17764	17545	17008	15447	15441
R11000F9D	10587	10438	10062	9189	7680	7677
R1100F1D	43898	43259	42036	38420	26785	26597
R1100F3D	31053	30601	29841	27756	22035	21989
R1100F4D	28685	28280	27281	24189	19239	19185
R1100F5D	44317	43708	42336	38300	27861	27820
R1100F6D	29577	29188	28438	25964	19406	19374
R1100F7D	34935	34497	33604	30873	23653	23598
R1100F8D	39662	39147	38233	35030	26933	26826
R1100F9D	35455	34972	33934	30656	21344	21285
R110F10D	34190	33693	32889	30368	25663	25609
R110F1D	21972	21697	21197	19621	15677	15664
R110F2D	14952	14739	14383	13384	11211	11208
R110F3D	8050	7952	7802	7367	6896	6866
R110F4D	42845	42260	41227	38024	27518	27355
R110F5D	13815	13625	13159	11694	9021	9010
R110F6D	8209	8077	7936	7490	6903	6895
R110F8D	33780	33259	32438	29886	24788	24722
R110F9D	10	8	2	2	2	2
R11F10D	28765	28385	27741	25751	21426	21388
R11F1D	29879	29489	28828	27067	21454	21359
R11F2D	18	16	6	5	5	5
R11F3D	13048	12883	12802	12690	12528	10974
R11F4D	38155	37693	37092	35137	27674	27604
R11F5D	39979	39464	38901	37153	31085	30999
R11F6D	18	15	4	4	4	4

sample	sequenced	filtered	denoised	merged	non-chimeric	bacteria only
R11F7D	43702	43144	42327	39722	33213	33107
R11F8D	35553	35123	34584	32811	28066	27971
R11F9D	18616	18358	17794	16362	13725	13672
R1CTRLF10D	13903	13659	13357	12641	11313	11311
R1CTRLF1D	33772	33184	32672	31076	27971	27949
R1CTRLF2D	16077	15860	15208	13726	11426	11379
R1CTRLF3D	37654	37198	36710	35424	32097	32086
R1CTRLF4D	26460	26084	24924	21133	17539	16981
R1CTRLF5D	30021	29557	28828	26582	21724	21688
R1CTRLF6D	10612	10363	10027	8880	8102	8079
R1CTRLF7D	29491	29066	28495	26785	22104	22007
R1CTRLF8D	1470	1433	1341	1273	1230	1230
R1CTRLF9D	19014	18642	18270	16856	15491	15281
R21000F10D	26634	26276	25955	24868	22882	22864
R21000F1D	37544	37055	36576	34646	28700	28660
R21000F2D	31102	30705	29731	26490	19163	19027
R21000F4D	35768	35319	34463	31618	20538	20488
R21000F5D	26219	25906	25348	23261	16013	15880
R21000F6D	8	5	1	0	0	0
R21000F8D	43340	42826	42150	39498	25869	25766
R21000F9D	33461	33005	32220	29226	20045	19960
R2100F10D	14	7	1	0	0	0
R2100F1D	189	177	152	142	142	142
R2100F2D	33965	33529	32813	30607	25113	25103
R2100F3D	31902	31011	30426	28789	21133	20885
R2100F5D	33388	32950	32352	30824	24409	24364
R2100F7D	35949	35413	34599	32274	26667	26634
R2100F8D	36925	36414	35751	34078	28240	28050
R210F10D	5298	5221	5154	4970	4347	4248
R210F12D	18679	18448	18307	17678	13917	13806
R210F1D	34098	33618	33037	31008	25465	25456
R210F3D	23251	22924	22486	21252	18233	18229
R210F4D	32841	32421	31886	29821	20698	20654
R210F5D	36028	35605	35152	33732	23110	22749
R210F6D	41810	41276	40330	37680	31249	31179
R210F7D	37388	36922	36339	34345	23449	23272
R210F8D	30929	30509	29394	26532	21086	20965
R210F9D	26952	26583	24992	19960	13252	13134
R21F10D	34123	33676	32785	29814	20214	20065

sample	sequenced	filtered	denoised	merged	non-chimeric	bacteria only
R21F1D	33629	33229	32624	30757	19448	19191
R21F2D	24195	23893	23439	21877	18393	18373
R21F3D	16267	14868	14641	13464	11733	10273
R21F5D	27110	26698	25733	22621	16307	16057
R21F6D	28127	27793	27344	25662	17195	17058
R21F7D	28397	28021	27659	26393	22659	22636
R21F8D	34782	34341	33180	30067	23286	23266
R21F9D	30093	29753	29532	28952	20128	16178
R2CTRLF10D	40173	39635	38774	35994	27074	26539
R2CTRLF1D	31	5	1	0	0	0
R2CTRLF2D	35690	35274	34447	31624	24248	24098
R2CTRLF3D	96	88	74	70	68	68
R2CTRLF4D	30654	30272	29914	28893	25424	25416
R2CTRLF5D	37700	37251	36776	35102	28721	28687
R2CTRLF7D	33363	32945	32245	29951	24715	24626
R2CTRLF8D	37737	37252	36184	33047	22901	22785
R2CTRLF9D	32345	31846	30092	23719	15740	13311
R31000F10D	5134	5030	4881	4546	4057	4056
R31000F1D	29779	29262	28954	28137	26197	26159
R31000F2D	88	41	1	0	0	0
R31000F3D	23779	23445	23001	21863	19548	19448
R31000F4D	36202	35616	34772	32009	25881	25407
R31000F5D	1363	1334	1283	1191	1184	1182
R31000F6D	31470	31059	30870	30342	26761	26441
R31000F7D	28007	27605	26989	25430	21549	21526
R31000F8D	17612	17253	17056	16621	15768	15731
R31000F9D	34138	33575	33183	32269	28318	28306
R3100F1D	36683	36137	35740	34692	31262	31208
R3100F2D	29681	29098	28894	28181	27662	16746
R3100F3D	34886	34371	33819	32023	26378	26352
R3100F4D	1135	594	497	459	459	202
R3100F5D	2087	2033	1929	1768	1705	1692
R3100F6D	26512	25568	25457	25258	25184	20550
R3100F7D	18421	16971	16812	16410	16073	12218
R3100F8D	20364	19953	19370	17981	14989	14982
R3100F9D	26781	26420	26280	25966	24224	24197
R310F10D	44	25	5	5	5	5
R310F1D	28751	28387	27580	25150	19952	19905
R310F2D	12459	12176	11993	11711	11080	11080

sample	sequenced	filtered	denoised	merged	non-chimeric	bacteria only
R310F3D	36440	35946	34868	31865	25590	25339
R310F4D	33567	33043	32372	30241	23391	23354
R310F5D	24745	24427	24098	23016	20549	20482
R310F6D	6650	6536	6384	6174	5773	5770
R310F7D	37	36	23	21	21	21
R310F8D	104	84	39	35	35	27
R310F9D	30553	30155	29592	27760	25368	25268
R31F10D	32904	32422	31552	28801	20181	20157
R31F1D	29987	29436	28802	26672	21926	21916
R31F2D	20212	19879	19598	18900	17216	17214
R31F3D	25492	25122	24348	21880	15622	15570
R31F4D	41450	40898	39855	36432	26684	26538
R31F5D	35381	34957	34208	31252	23189	23118
R31F6D	4938	4804	4694	4478	4231	4225
R31F7D	34032	33550	32629	29466	22426	22352
R31F8D	6110	6008	5901	5676	5233	5233
R31F9D	32479	31898	30841	27627	20337	20306
R3ContF10D	23776	23424	22929	21408	17630	17598
R3ContF1D	22425	22122	21545	20059	16922	16914
R3ContF2D	34475	33940	33036	30195	23544	23341
R3ContF3D	31928	31542	30659	27440	21189	21138
R3ContF4D	40813	40245	39134	35765	27974	27922
R3ContF5D	52	32	4	4	4	4
R3ContF6D	36224	35702	34681	31672	24333	24165
R3ContF7D	28595	28170	27358	25048	20325	20306
R3ContF8D	32153	31698	30675	27429	20396	20328
R3ContF9D	34758	34213	33167	29857	22128	22115
R1100F5xD	27855	27437	26923	25381	21244	21148
R11F7xD	69315	68451	67156	62550	46406	46075
R21000F2xD	47439	46427	45531	42317	29519	29367
R2100F8xD	3	3	2	0	0	0
R2CTRLF4xD	28104	27731	26670	23549	15624	15501
R31F10xD	39858	39337	38236	35397	27388	27222

101

Table S3. Concentrations of benzo[*a*]pyrene (BaP) in food and metabolites of BaP in bile. Reported as mean ± standard errors (SE).

Nominal Exposure $\mu g\ g^{-1}$	**Food** $\mu g\ g^{-1}$	**OH-BaP** $ng\ g^{-1}$	**BaP-Gluc** $ng\ g^{-1}$	**BaP-SO_4** $ng\ g^{-1}$	**Sum** $ng\ g^{-1}$
0	0.06 ± 0.02	0.00 ± 0.00	0.00 ± 0.00	178 ± 51.3	165 ± 45.5
1	0.98 ± 0.04	0.00 ± 0.00	1.44 ± 1.44	46.7 ± 17.9	53.7 ± 19.6
10	8.03 ± 1.61	0.00 ± 0.00	9.63 ± 2.88	1,390 ± 308	1,437 ± 266
100	104 ± 3.08	7.67 ± 3.32	157 ± 46.9	8,080 ± 2,280	9,651 ± 2,468
1,000	1,170 ± 32.1	49.0 ± 16.7	280 ± 92.6	41,000 ± 9,560	51,071 ± 9,403

Table S4. Parameters of co-association gut microbial network.

Nominal Exposure $\mu g\ g^{-1}$	**Number of nodes**	**Number of edges**	**Avg. number of neighbors**	**Cluster coefficient**	**Network heterogeneity**	**Network centralization**
0	107	544	12.364	0.557	0.793	0.337
1	89	240	7.045	0.499	0.655	0.202
10	80	583	14.048	0.591	0.648	0.249
100	78	332	9.735	0.555	0.57	0.189
1000	81	127	4.593	0.435	0.611	0.145

Supplemental Figures:

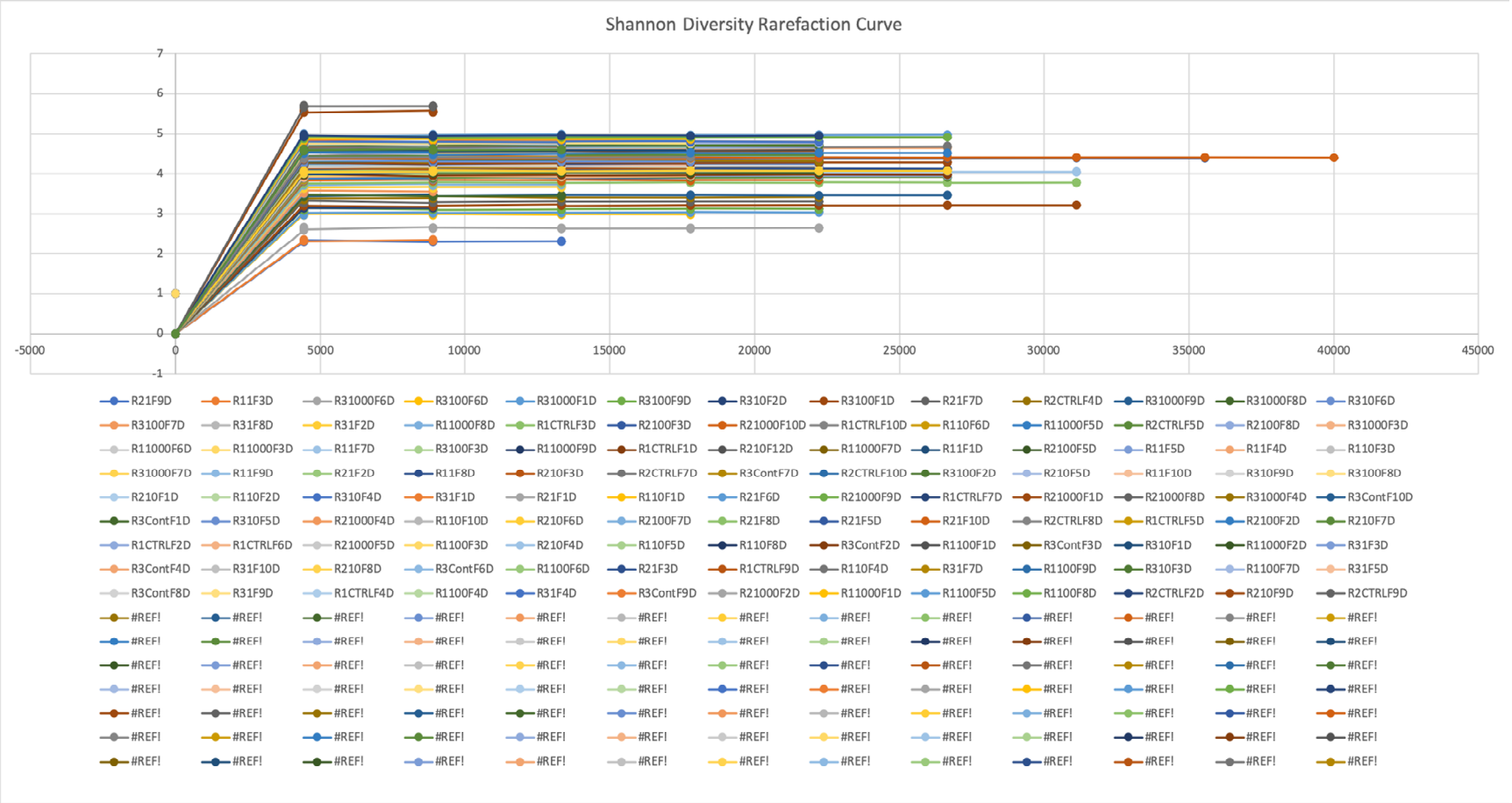

Fig. S1. Rarefaction curve of Shannon Diversity values across sequencing depths.

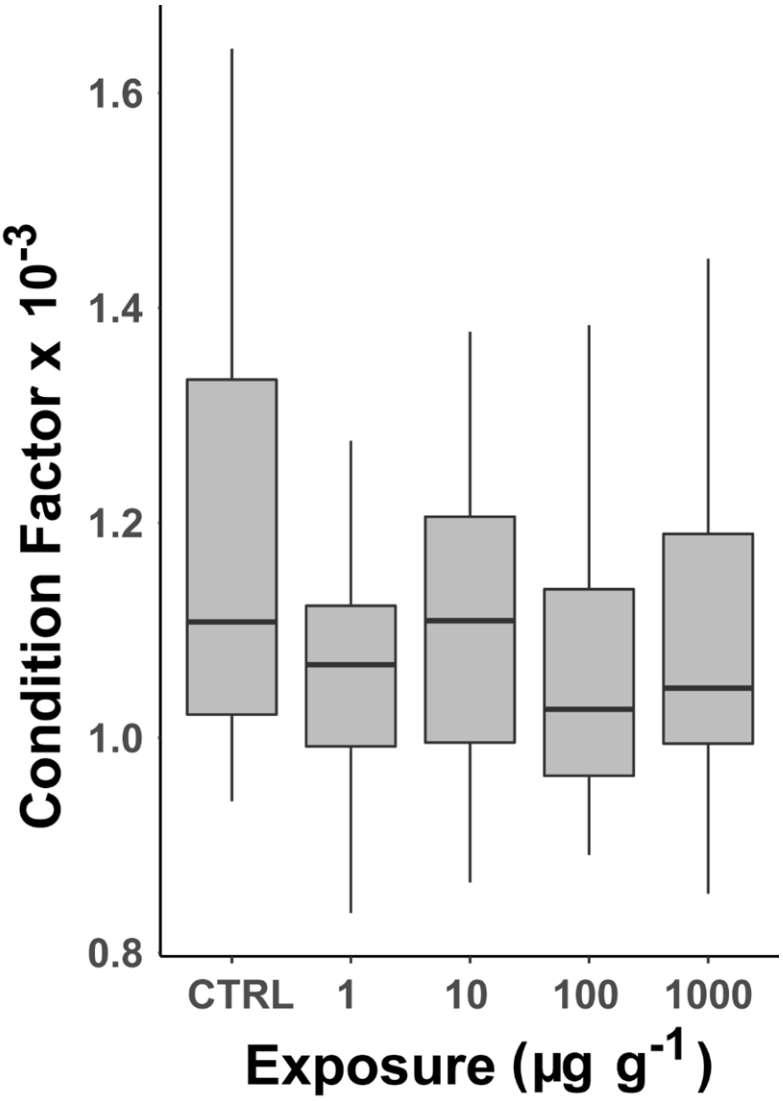

111

112 Fig. S2. Condition factor of fish exposed to BaP within each exposure group. Exposure did not

113 significantly affect the condition factors of these fish.

114
115

116 A.

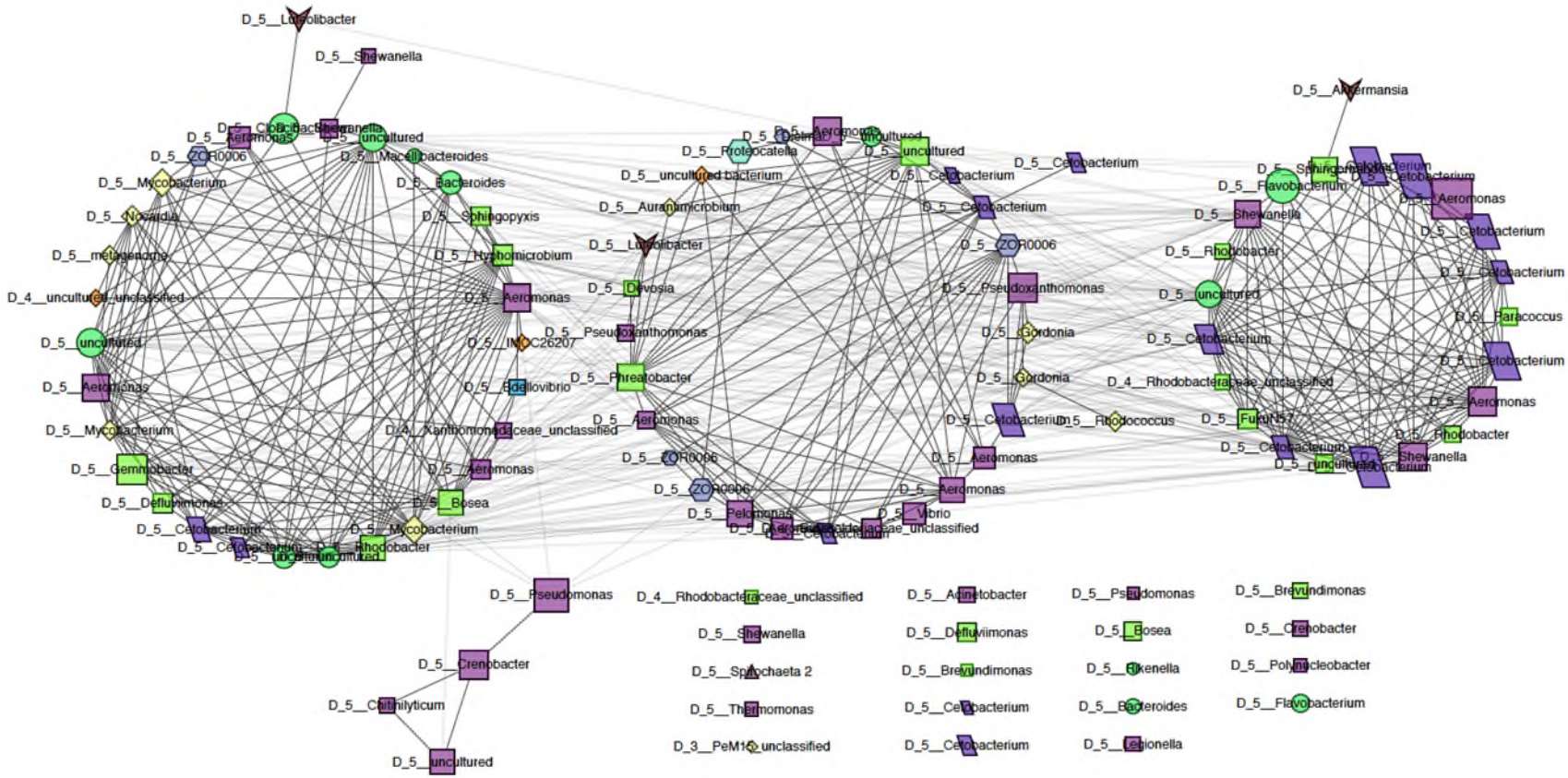
D_5__Luteolibacter
D_5__Shewanella
D_5__Aeromonas
D_5__uncultured
D_5__ZOR0006
D_5__Mycobacterium
D_5__Nocardia
D_5__metagenome
D_4__uncultured_unclassified
D_5__uncultured
D_5__Aeromonas
D_5__Mycobacterium
D_5__Gemmobacter
D_5__Defluviimonas
D_5__Cetobacterium
D_5__Rhodobacter
D_5__Mycobacterium
D_5__Bosea
D_5__Aeromonas
D_4__Xanthomonadaceae_unclassified
D_5__Bdellovibrio
D_5__IMCC26207
D_5__Pseudoxanthomonas
D_5__Mycobacterium
D_5__Bacteroides
D_5__Sphingopyxis
D_5__Hyphomicrobium
D_5__Aeromonas
D_5__Pseudomonas
D_5__Crenobacter
D_5__Caldilyticum
D_5__uncultured
D_4__Rhodobacteraceae_unclassified
D_5__Shewanella
D_5__Spirochaeta 2
D_5__Thermomonas
D_3__PeM15_unclassified
D_5__Actinetobacter
D_5__Defluviimonas
D_5__Brevundimonas
D_5__Cetobacterium
D_5__Cetobacterium
D_5__Pseudomonas
D_5__Bosea
D_5__Rikenella
D_5__Bacteroides
D_5__Legionella
D_5__Brevundimonas
D_5__Crenobacter
D_5__Polymorphobacter
D_5__Flavobacterium
D_5__Akkermansia
D_5__Flavobacterium
D_5__Shewanella
D_5__Rhodobacter
D_5__uncultured
D_5__Cetobacterium
D_4__Rhodobacteraceae_unclassified
D_5__Fukuin57
D_5__Cetobacterium
D_5__Paracoccus
D_5__Aeromonas
D_5__Rhodobacter
D_5__Shewanella
D_5__Cetobacterium
D_5__Cetobacterium
D_5__Cetobacterium
D_5__Cetobacterium
D_5__uncultured bacterium
D_5__Auranticimicrobium
D_5__Luteolibacter
D_5__Devosia
D_5__Phreatobacter
D_5__Aeromonas
D_5__ZOR0006
D_5__ZOR0006
D_5__Pelomonas
D_5__Vibrio
D_5__Aeromonas
D_5__Gordonia
D_5__Gordonia
D_5__Cetobacterium
D_5__Rhodococcus
D_5__Aeromonas
D_5__Pseudoxanthomonas
D_5__ZOR0006
D_5__Cetobacterium
D_5__Cetobacterium
D_5__Cetobacterium
D_5__uncultured
D_5__Proteocatella
D_5__Aeromonas
D_5__uncultured

117

B.

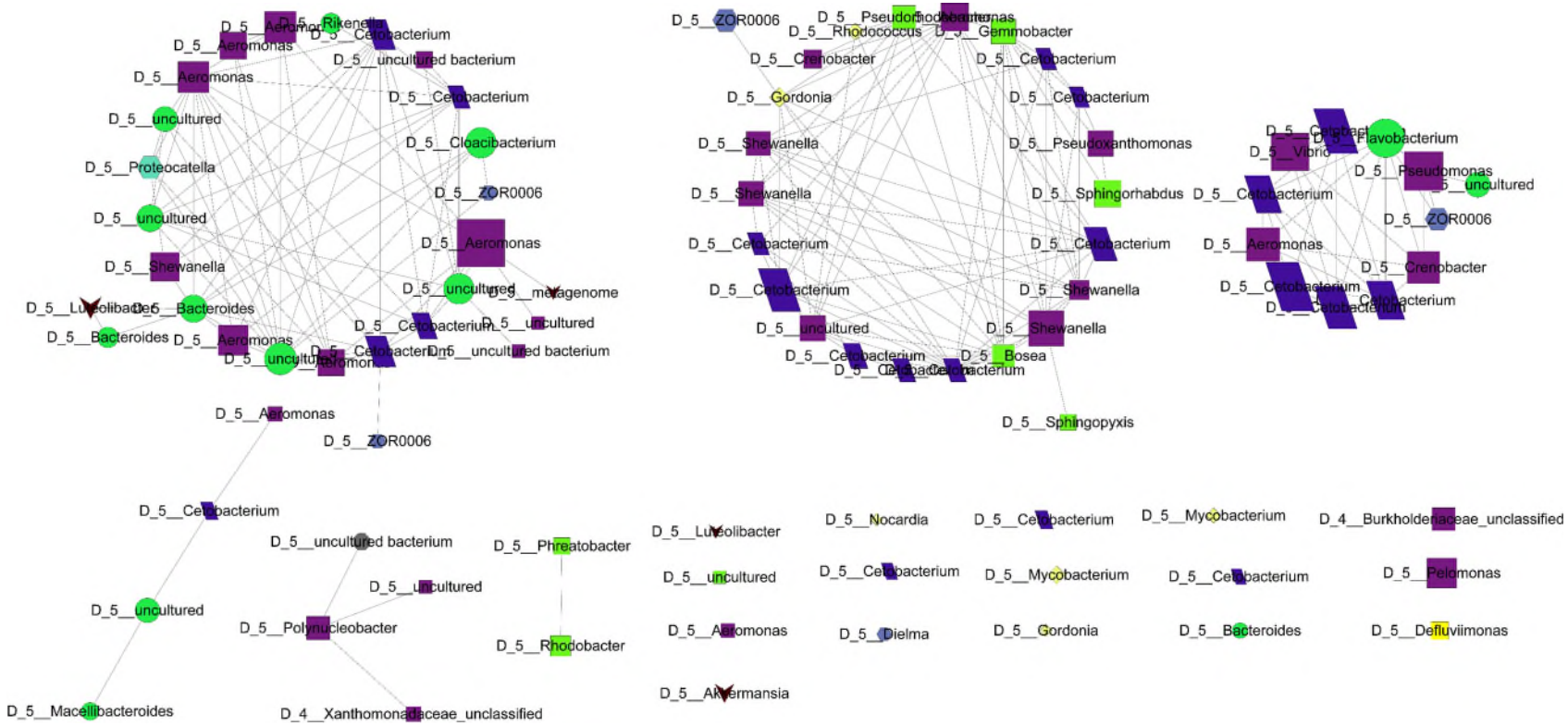
D_5__Aeromonas
D_5__Cetobacterium
D_5__uncultured bacterium
D_5__uncultured
D_5__Cloacibacterium
D_5__Proteocatella
D_5__ZOR0006
D_5__Shewanella
D_5__Bacteroides
D_5__metagenome
D_5__Macellibacteroides
D_5__Phreatobacter
D_5__Polynucleobacter
D_5__Rhodobacter
D_4__Xanthomonadaceae_unclassified
D_5__Gordonia
D_5__Pseudoxanthomonas
D_5__Sphingorhabdus
D_5__Bosea
D_5__Sphingopyxis
D_5__Vibrio
D_5__Flavobacterium
D_5__Pseudomonas
D_5__Crenobacter
D_5__Nocardia
D_5__Mycobacterium
D_4__Burkholderiaceae_unclassified
D_5__Pelomonas
D_5__Dielma
D_5__Defluviimonas

120 C.

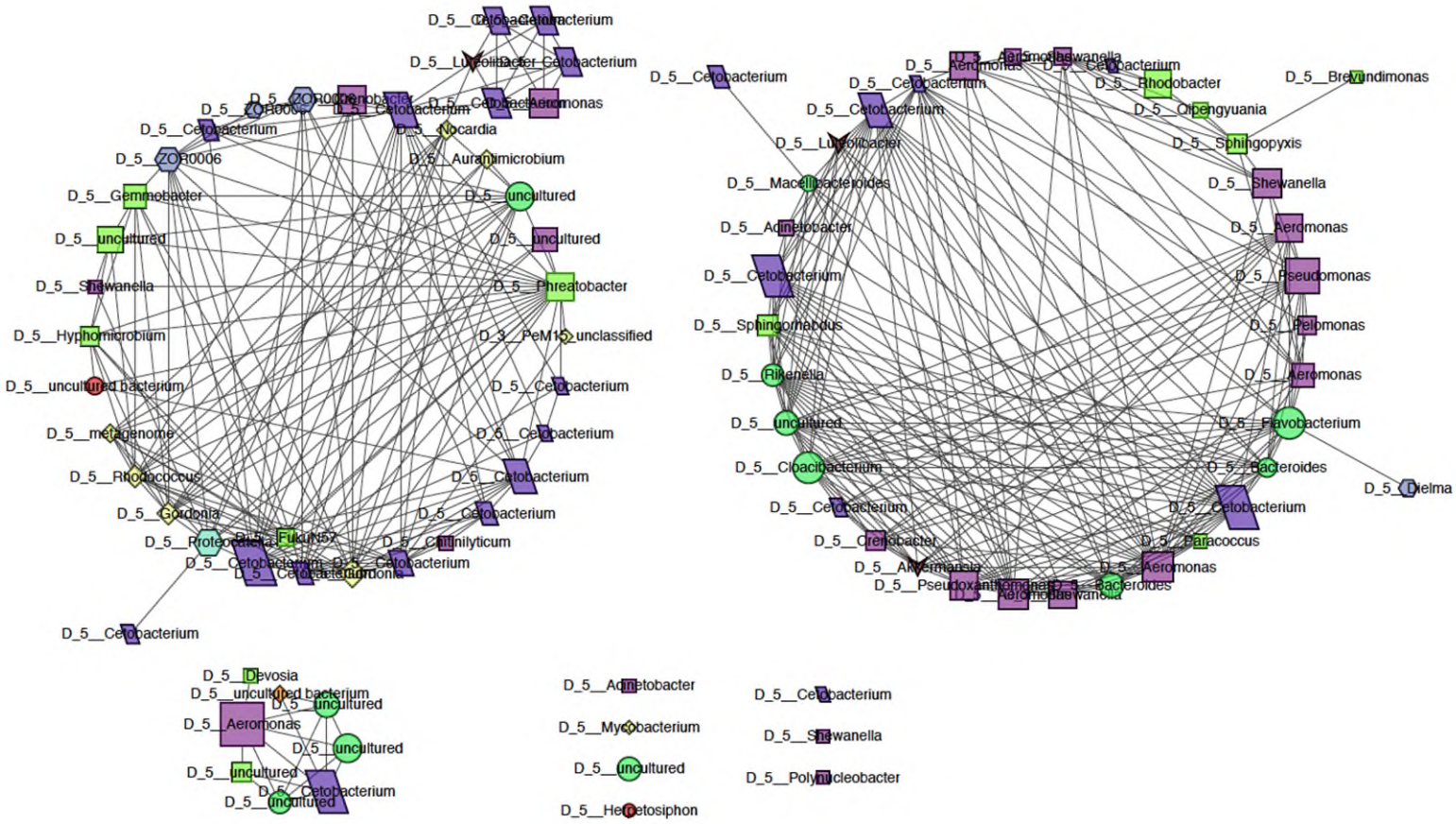
D_5__Cetobacterium
D_5__Lucibacter
D_5__ZOR0006
D_5__Nocardia
D_5__Aurantimicrobium
D_5__Gemmobacter
D_5__uncultured
D_5__Shewanella
D_5__Phreatobacter
D_5__Hyphomicrobium
D_3__PeM15_unclassified
D_5__uncultured bacterium
D_5__metagenome
D_5__Rhodococcus
D_5__Gordonia
D_5__Proteocatella
D_5__Fusibacter
D_5__Clostridium
D_5__Aeromonas
D_5__Rhodobacter
D_5__Qipengyuania
D_5__Sphingopyxis
D_5__Macellibacteroides
D_5__Acinetobacter
D_5__Pseudomonas
D_5__Sphingomonadus
D_5__Rikenella
D_5__Flavobacterium
D_5__Cloacibacterium
D_5__Bacteroides
D_5__Dielma
D_5__Crenobacter
D_5__Paracoccus
D_5__Devosia
D_5__Mycobacterium
D_5__Herbetosiphon
D_5__Polynucleobacter

121

122 D.

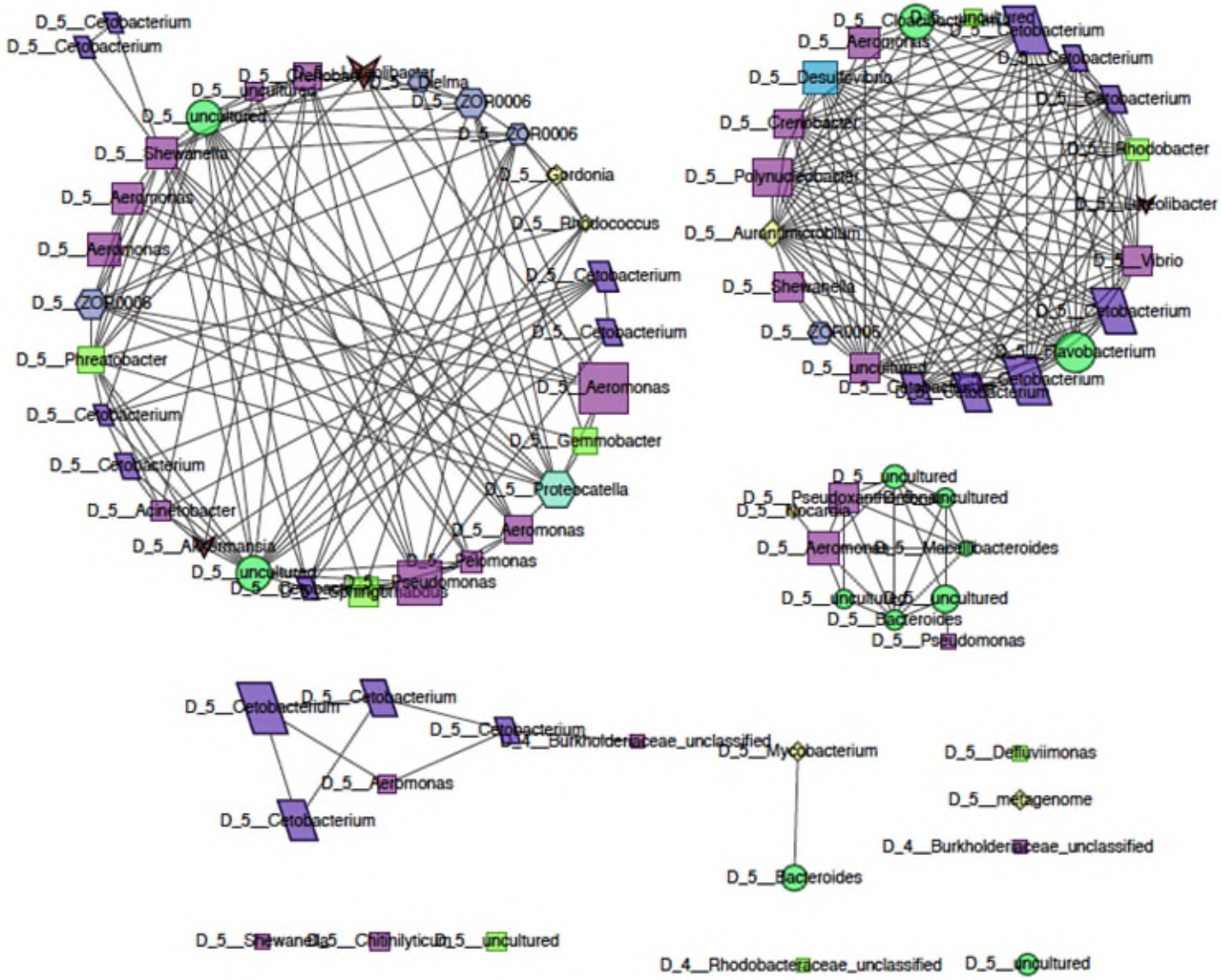
D_5__Cetobacterium
D_5__Cetobacterium
D_5__uncultured
D_5__Shewanella
D_5__Aeromonas
D_5__Aeromonas
D_5__ZOR0006
D_5__Phreatobacter
D_5__Cetobacterium
D_5__Cetobacterium
D_5__Acinetobacter
D_5__Aeromonas
D_5__Pseudomonas
D_5__ZOR0006
D_5__Gordonia
D_5__Rhodococcus
D_5__Cetobacterium
D_5__Cetobacterium
D_5__Aeromonas
D_5__Gemmobacter
D_5__Proteocatella
D_5__Aeromonas
D_5__Cetobacterium
D_5__Cetobacterium
D_5__Aeromonas
D_5__Cetobacterium
D_5__Desulfovibrio
D_5__Crenobacter
D_5__Polynucleobacter
D_5__Aurantimicrobium
D_5__Shewanella
D_5__ZOR0006
D_5__Rhodobacter
D_5__Vibrio
D_5__Cetobacterium
D_5__Flavobacterium
D_5__uncultured
D_5__uncultured
D_5__Pseudoxanthomonas
D_5__Nocardia
D_5__Aeromonas
D_5__Bacteroides
D_5__Pseudomonas
D_5__Cetobacterium
D_5__Cetobacterium
D_5__Cetobacterium
D_5__Aeromonas
D_5__Cetobacterium
D_5__Mycobacterium
D_5__Deinococcus
D_5__metagenome
D_4__Burkholderiaceae_unclassified
D_5__Bacteroides
D_5__Shewanella
D_5__Chitinilyticum
D_5__uncultured
D_4__Rhodobacteraceae_unclassified
D_5__uncultured

123

E.

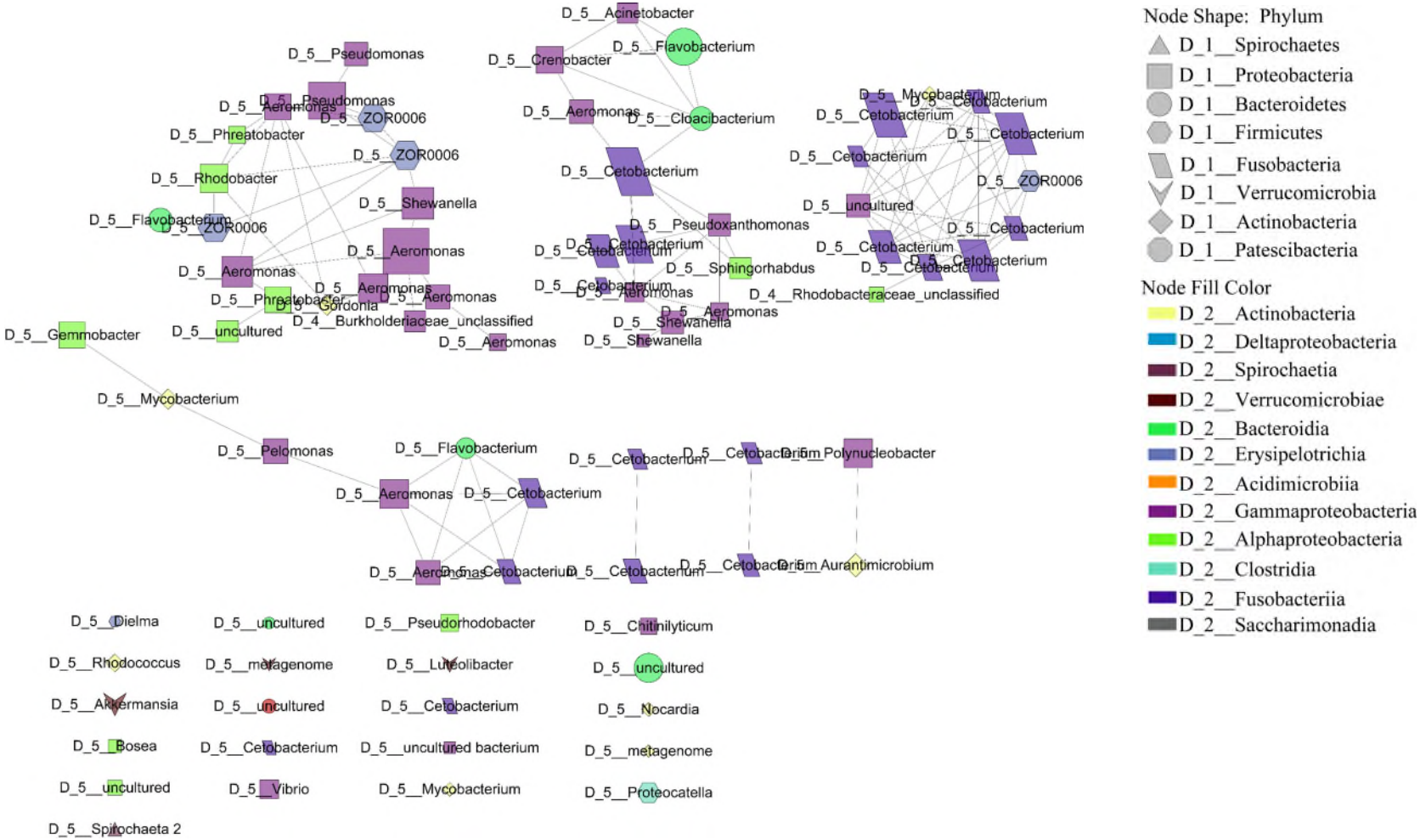

Fig. S3. Association networks generated through SparCC assembled at the level of genera for (A) Control, (B) 1, (C)10, (D) 100, and (E) 1000 µg g^{-1}.